IEEE Access
Multidisciplinary | Rapid Review | Open Access Journal

Received June 18, 2020, accepted July 3, 2020, date of publication July 16, 2020, date of current version July 29, 2020.

*Digital Object Identifier 10.1109/ACCESS.2020.3009778*

# Semi-Decentralized Interference Aware Scheduling in D2D-Enabled Cellular Networks

**MARKUS KLÜGEL, (Member, IEEE), AND WOLFGANG KELLERER, (Senior Member, IEEE)**
Chair of Communication Networks, Technical University of Munich, 80333 München, Germany
Corre sponding author: Markus Klügel (markus.kluegel@tum.de)

**ABSTRACT** We investigate the problem of semi-decentralized, interference aware scheduling in a cellular network with Device-to-Device (D2D) links. Our goal is an algorithm that allows optimal resource allocation and power control in spite of mutual interference from and to D2D links, as well as the creation of a reporting structure that is independent of the exact optimization goal and D2D modes. To achieve this, we formulate an interference aware scheduling problem with general rate-utility and generalized reuse constraints. By applying a Generalized Benders Decomposition, the problem is decomposed into two coupled sub-problems, a ''primal'' power control problem and a ''master'' scheduling problem, that can be dealt with independently. By this, we decouple the tedious power optimization from the scheduling part. We evaluate performance of the proposed structure analytically and find it to allow optimal scheduling independent of the used utility and D2D modes, provided that the master scheduling problem is solved optimally. Finally, we propose a solution for the master problem of weighted sum-rate maximization. Our simulations indicate that using the proposed scheme, D2D reuse can increase by an order of magnitude compared to the often targeted one-fold reuse, reaching a maximum of 31-fold frequency reuse in our set-ups. It is further capable of improving sum-rate performance by around 35% over existing works, while keeping signaling overhead and optimization delay at the same order of magnitude.

**INDEX TERMS** Device-to-Device, D2D, 5G, interference management, frequency reuse, power control, scheduling.

## I. INTRODUCTION

Direct communication among user equipments (UEs) is envisioned to enhance future cellular networks. Such direct communication, referred to as Device-to-Device (D2D) communication, is considered to offload spatially local traffic from the cellular base station and has received increased attention among network researchers [1], [2]. One of the potential benefits is that D2D communication can leverage the proximity of devices to perform dynamic frequency reuse, which allows pushing the frequency reuse factor beyond one [3]. However, the management of dynamic frequency reuse is a challenging task, due to intracell interference added to the system.

Frequency reuse by D2D links has attracted much attention in academia. The often taken perspective is to treat cellular uplinks as primary users, whose channels may be reused by D2D sidelinks as long as the uplink transmissions are not disturbed too much. To ensure the quality of uplink transmissions, the employed techniques include aspects of power control, scheduling and reuse link pairing, i.e., identification of appropriate links to share a channel.

Because the full optimization over all available parameters often creates mixed-integer nonlinear problem (MINLP) structures, which are considered intractably complex for the D2D set-up, simplifications are used in the respective literature, such as fixing transmission powers or restricting reuse to at most one D2D link per channel. However, while these restrictions ease the management effort, they also limit the performance potential of D2D communication. Previous works [4]–[7], show that up to 40-fold frequency reuse in a cell can be achieved if these limitations are lifted. Although the exact number depends on many parameters, such as the cell size, average link distance and targeted Signal to Interference and Noise Ratio (SINR), the conclusion is that frequency reuse could in fact be by orders of magnitude larger than often targeted in research. The main enabler for this large number of reuses seems to be dynamic power control, which adapts the transmission powers to the current interference situation. Unfortunately, to unleash the full potential of D2D-reuse, a complex interference aware scheduling problem must be solved with power control and without any simplifying

The associate editor coordinating the review of this manuscript and approving it for publication was Meng-Lin Ku.

restrictions. How to do so in an efficient and implementable manner is investigated in this article.

In this work, we apply a Generalized Benders Decomposition (GBD) to an interference aware D2D scheduling problem including full power control and allowing an arbitrary amount of reuse. The result is a two-stage management structure with low communication overhead, in which part of the parameters are optimized decentrally, effectively taking the burden off the base station while still allowing optimal parameter choice. A scheduling problem remains that may be adapted to the specific needs of the operator and that can be solved with conventional methods. We show with simulations that our proposed solution can enable frequency reuse in an order of magnitude around 30 times per cell, which goes far beyond the often targeted one-fold reuse of underlay communication. Further, we are able to give mathematical pre-requisites for optimality of the resulting schedule. Due to the generality of our formulation, the results are applicable to a variety of problem cases, including reuse in uplink or downlink bands or solely among D2D-links and including one-fold or multi-fold reuse of a channel.

### A. RELATED WORK AND CONTRIBUTION

Interference management in the context of underlay D2D communication creates an interesting interplay of traditional power control problems [8] and mixed-integer scheduling problems. Additional flavor is added by the network setup, which is characterized by a lack of central parameter knowledge such that the use of fully centralized solutions is disadvantageous. The combination of these properties has led to a number of research works that we discuss at this point.

A series of works deal with interference management for D2D links [9]–[25], each of which targets a slightly different system model or problem target. For example, the works differ in whether downlink bands [11], [19] or uplink bands [9], [10], [12]–[18], [20]–[25] are considered, in whether fixed transmission powers are assumed [9], [12], [13], [22]–[24] or power control is part of the optimization [10], [11], [14]–[21], [25], whether frequency reuse is constrained to one-fold reuse by D2D links [9]–[11], [14], [18], [20], [25] or multiple D2D links may use the same frequency [12], [13], [15]–[17], [19], [21]–[24], or in the optimization target, which typically is assumed to be the sum-rate [9], [10], [12], [13], [16]–[23], [25] but can also be proportional fair rate [24], a general utility [11] or just the satisfaction of rate constraints [15]. Due to the complexity of the considered problem, various solutions have been proposed, each tailored to another special case and dependent on the particular assumptions of the specific investigated system. Unfortunately, many of these solutions have incompatible reporting structures, as they require different levels and amount of information. Further, surprisingly many solutions rely on explicit channel knowledge, which however is inefficient to obtain. In this work we try to ease these constraints by proposing an efficient reporting structure that may be applied to various use-cases, while preserving the opportunity to achieve an optimal resource allocation.

The work closest related to ours is in the field of multi-fold reuse with dynamic power control, for which we find [15]–[17], [21]. In [16], Zhao and Wang propose the use of an alternating optimization, switching between a greedy resource allocation and an interference management that is solved for fixed allocation using the method of differences of convex functions. The result is a centralized scheme that outperforms that of Feng *et al.* [10]. Zhao and Wang also propose a three-stage optimization in [17]. In the first stage, they construct a method to identify D2D-pairs that will cause too much harm when reusing a channel at the same time. Then, resources are allocated with a greedy approach and powers are assigned by neglecting mutual interference among D2D links, resulting in a waterfilling solution. Again, the scheme is centralized. Yin *et al.* [15], [21] investigate decentralized pricing schemes for multi-fold D2D-reuse with power control, to find an allocation that satisfies D2D rate constraints [15] and maximizes D2D sum-rate [21] while protecting uplinks from interference. They formulate a Stackelberg game with the base station as leader, having the goal of protecting the data rates of the uplinks by an interference price, and the D2D-links trying to satisfy their constraints or maximizing their rate. The result is in both cases an iterative waterfilling algorithm for the D2D-users and a pricing mechanism at the base station (BS).

Note that more related work exists for multi-fold reuse without power control [12], [13], [22], [23] and one-fold reuse with power control [10], [11], [14], [18]–[20], [25]. However, fixed powers yield a completely different, simpler problem that is purely combinatorial. One-fold reuse, on the other hand, significantly limits D2D performance and is also simpler, because optimal power allocations can be explicitly enumerated for each reuse pair, which is leveraged, e.g., in [10], [14], [18], [19], [25].

Our work differs from the ones mentioned for multi-fold D2D reuse with dynamic power control already in the used model and problem formulation. In contrast to [15]–[17], [21], we optimize towards a general rate-utility instead of the sum-rate, do not use the Shannon bound approximation for rate but include Modulation and Coding Scheme (MCS) selection explicitly into the problem. Compared to [16], [17], we provide a solution that can solve the problem optimally or with well-defined performance bounds. Further, our solution can be readily applied to various D2D scenarios, to one-fold and multi-fold reuse, with or without rate constraints and adjacency constraints for frequencies.

We have investigated similar problems to the one presented here in previous works [4], [5], [26], [27]. In [4], [5], [26], we investigated the Reuse Maximization Problem (RMP), i.e., the problem of how to maximize the number of reusing D2D links on a single transmission resource, with the most promising result being a GBD-based solution. Compared to these works, in which we maximized the reuse factor, we here investigate the problem of rate-utility maximization, which is significantly different and more complex. The idea of transferring the general concept of the GBD-based solution [5] to

a utility maximization is briefly discussed in [26] with initial simulation results presented in [27]. However, this article significantly enhances both works by formally developing Algorithm 1, analyzing it analytically in Section IV and by largely augmenting the simulation results in Section V.

### B. CONTRIBUTIONS OF THIS WORK

In this work, we investigate an interference-aware rate-utility maximization problem for D2D communication. Our contributions can be summarized as follows:

- We investigate a rate-utility maximization problem in a very general form. This makes it harder to solve but also makes it powerful, because the results can be transferred to D2D communication underlaying uplink or dowlink bands or network slices, to D2D links that share a slice in an overlay fashion, to problems with one-fold or multi-fold reuse and to problems with general rate constraints and resource restrictions.
- We propose a semi-distributed structure that splits power control from the scheduling problem. This reduces complexity significantly, as it avoids tedious power optimization alongside scheduling.
- Our solution can be implemented relying only on SINR measurements, avoiding the overhead of full channel reporting.
- The structure allows provenly optimal resource allocation for all set-ups contained in our model, provided that the scheduling problem is optimally solved. For sub-optimal solutions, we provide performance bounds.
- With simulations, we show that the same method can be applied to different types of reuse. Compared to one-fold reuse, we are able to increase the system rate by a factor of seven and the average frequency reuse by a factor of 18. Compared to existing works, we are able to increase the sum-rate by around 35%.
- We show-case the applicability to varying channel conditions with simulations.

### C. MATHEMATICAL NOTATIONS

In this article, the following mathematical notations are used: Lower case, Greek or Roman letters $a$ denote scalars, whereas bold, lower case variables $\boldsymbol{a}$ are used for column vectors and matrices $\boldsymbol{A}$ are described with upper case, bold letters. Vector or matrix transposition is written as $(\cdot)^T$, i.e., $\boldsymbol{a}^T$, $\boldsymbol{A}^T$ are the transposed of $\boldsymbol{a}$ and $\boldsymbol{A}$. The $\ell^p$-norm of a vector is given as $\|\boldsymbol{a}\|_p = \sqrt[p]{\sum_i a_i^p}$. Functions or relations on vectors and matrices, e.g., $e^{\boldsymbol{a}}$, $\boldsymbol{a} \leq \boldsymbol{b}$ are to be interpreted element-wise.

Calligraphic upper case letters, e.g., $\mathcal{A}$, are used for general sets, whereas the set of real numbers is given by $\mathbb{R}$ and that of integers by $\mathbb{N}$. The latter two are restricted to non-negative numbers by $\mathbb{R}_+$, $\mathbb{N}_+$, respectively. The expression $2^{\mathcal{A}}$ refers to the power set of $\mathcal{A}$, which is the set of subsets of $\mathcal{A}$.

The function $\mathbb{1}\{\cdot\}$ denotes the indicator function, which is one if the expression in the brackets is true and zero otherwise. Finally, the expression $[\boldsymbol{a}]^+ = \max\{\boldsymbol{a}, 0\}$ projects a vector to the non-negative orthant.

An overview over used variables and their meanings is given in Table 1.

**TABLE 1. Used variables and their meanings.**

| Variables | Meanings |
|---|---|
| $\mathcal{N}$ | Set of nodes |
| $\mathcal{L}; L; i \in \mathcal{L}$ | Set of links; number of links; link index |
| $\mathcal{R}; \mathcal{R}_i; k \in \mathcal{R}$ | Set of PRBs; Allowed PRBs for link $i$; PRB index |
| $p_i^{(k)}; \boldsymbol{p}_i; \boldsymbol{p}$ | Power of link $i$ on PRB $k$; power vector of $i$; overall power vector |
| $\overline{p}_i^{(k)}; \overline{\boldsymbol{p}}_i; \overline{\boldsymbol{p}}$ | Max. power constraints |
| $h_{ij}^{(k)}$ | Channel attenuation from link $j$ to $i$ on PRB $k$ |
| $\sigma_i^{(k)}$ | Receiver noise of link $i$ on PRB $k$ |
| $\Gamma_i^{(k)}(\boldsymbol{p})$ | SINR of link $i$ on PRB $k$ |
| $\gamma_{q_i}; \boldsymbol{\gamma}_i$ | SINR target of MCS $q_i \in \mathcal{X}_i$; target vector for $i$ |
| $\tilde{\boldsymbol{p}}; \tilde{\boldsymbol{\gamma}}$ | Log-transformation of $\boldsymbol{p}$; $\boldsymbol{\gamma}$; (e.g., $\tilde{\boldsymbol{p}} = \log(\boldsymbol{p})$) |
| $\mathcal{X}_i; q \in \mathcal{X}_i$ | Valid MCS for link $i$; MCS index |
| $x_{qi}^{(k)}; \boldsymbol{x}_i^{(k)}; \boldsymbol{x}_i$ | Indicator for use of MCS $q$ by link $i$ on PRB $k$<br>Indicator vector for link $i$ on PRB $k$ / for link $i$ |
| $\boldsymbol{x}$ | Global MCS indicator vector / scheduling vector |
| $d_{q_i}; \boldsymbol{d}_i; \boldsymbol{d}$ | Rate achieved by MCS $q_i \in \mathcal{X}_i$;<br>MCS rate vector for $i$; global MCS rate vector |
| $r_i^{(k)}; \boldsymbol{r}_i; \boldsymbol{r}$ | Rate achieved by link $i$ on PRB $k$; rate vector of $i$; global rate vector |
| $U_i(\boldsymbol{r}_i); U(\boldsymbol{r})$ | Utility function of link $i$; global utility function |
| $\boldsymbol{g}(\boldsymbol{x})$ | Vector of scheduling constraints |
| $\boldsymbol{h}(\boldsymbol{r})$ | Vector of rate constraints |
| $\zeta_k(\boldsymbol{x}, \boldsymbol{r})$ | $k$'th GBD master constraint function |
| $\xi_l(\boldsymbol{x}, \boldsymbol{r})$ | $l$'th GBD primal constraint function |

## II. SYSTEM MODEL AND PROBLEM FORMULATION

We consider a single cell[1] of a D2D-enabled cellular network, as is shown in Figure 1. The cell comprises of uplink, downlink and direct link connections that need to be scheduled for transmissions. Several time-frequency blocks, called Physical Resource Blocks (PRBs), are available for transmission and on each PRB, one out of a set of possible MCS needs to be chosen together with a transmission power. Each MCS is associated with a minimum SINR that needs to be satisfied in order to comply with a maximum block error rate. The network operator may define a set of scheduling constraints that limit the usable PRBs, the amount of reuse and guaranteed rate for cellular links. However, if allowed by the operator, any links may reuse a channel, as long as the respective SINR constraints associated with their desired MCS can be satisfied. In this setup, the target is to find optimal MCSs, transmission powers and PRB allocation to maximize a given rate-utility.

### A. SYSTEM MODEL

Formally, we model the network as a set of nodes $\mathcal{N}$, which are grouped into the set of transmission links $\mathcal{L} \in 2^{\mathcal{N}\times\mathcal{N}}$

[1] We assume that for larger scale networks, spectrum is partitioned in a way that inter-cell interference can be neglected, which leads to the optimization of several, independent single cells. Ways for extension towards multicell environments are discussed in Section V-D.

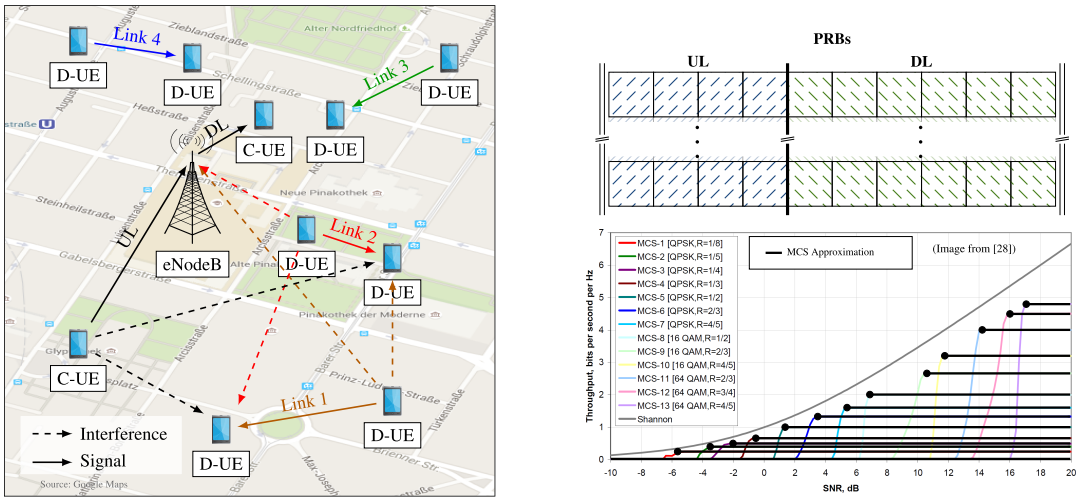


(a) (b)

**FIGURE 1.** Example setup of the D2D-enabled cellular network. We consider a network with given Physical Resource Block (PRB) structure that is divided into uplink and downlink partitions. Each link is assigned PRB resources and Modulation and Coding Schemes (MCSs), which provide a certain rate if certain SINR constraints are satisfied. The D2D links may reuse PRBs while causing interference with adaptive power control, however all SINR constraints of all links need to be satisfied.

containing $L = |\mathcal{L}|$ links in total. Note that $\mathcal{L}$ may include uplinks, downlinks and D2D links. The PRBs are given as a resource set $\mathcal{R}$ out of which each link $i \in \mathcal{L}$ is allowed to use a subset $\mathcal{R}_i \subseteq \mathcal{R}$. $\mathcal{R}_i$ can constrain PRB usage to uplink bands, downlink bands, dedicated D2D bands or a network slice. On each PRB $k \in \mathcal{R}$ a link may use one out of a set $\mathcal{X}_i$ of MCS for transmission, which it employs in combination with a transmission power $p_i^{(k)}$ on that resource. The transmission powers of link $i$ on the different PRBs are gathered in the column power vector $\boldsymbol{p}_i = [p_i^{(1)}, \ldots, p_i^{(|\mathcal{R}|)}]^T$ and all powers are gathered in the overall power vector $\boldsymbol{p} = [\boldsymbol{p}_1^T, \ldots, \boldsymbol{p}_L^T]^T$, respectively. Each links' power vector $\boldsymbol{p}_i$ is subject to maximum power constraints of the form $\boldsymbol{p}_i \leq \overline{\boldsymbol{p}}_i$, where the vector $\overline{\boldsymbol{p}}_i = [\overline{p}_i^{(1)}, \ldots, \overline{p}_i^{(|\mathcal{R}|)}]^T$.

The use of an MCS $q$ on PRB $k$ by link $i$ is indicated by variable $x_{qi}^{(k)} \in \{0, 1\}$, which is one if, and only if, the MCS is to be used. A scheduling decision is entirely reflected by the MCS choices, because links that are not scheduled for transmission on PRB $k$ simply satisfy $\sum_{q \in \mathcal{X}_i} x_{qi}^{(k)} = 0$. All $x_{qi}^{(k)}$ are gathered into a vector per link and PRB, $\boldsymbol{x}_i^{(k)} = [x_{1i}^{(k)}, \ldots, x_{|\mathcal{X}_i|i}^{(k)}]^T$, and further into a vector per link, $\boldsymbol{x}_i = [\boldsymbol{x}_i^{(1)T}, \ldots, \boldsymbol{x}_i^{(|\mathcal{R}|)T}]^T$, and an overall vector $\boldsymbol{x} = [\boldsymbol{x}_1^T, \ldots, \boldsymbol{x}_L^T]^T$, respectively. Depending on the transmission capabilities, each link is subject to a vector of scheduling constraints, given as $\boldsymbol{g}(\boldsymbol{x}) \leq \boldsymbol{0}$. These scheduling constraints are used to restrict resource usage in a fashion desired by the operator. In particular, they can capture that resource usage is restricted to uplink or downlink bands or network slices (e.g., if $\boldsymbol{g}(\boldsymbol{x})$ contains elements $g_i^{(k)}(\boldsymbol{x}) = \sum_{q \in \mathcal{X}_i} x_{qi}^{(k)} - \mathbb{1}\{k \in \mathcal{R}_i\}$ for appropriate $\mathcal{R}_i \subseteq \mathcal{R}$), that reuse is restricted to a certain number (e.g., if $\boldsymbol{g}(\boldsymbol{x})$ contains elements $g_r^{(k)}(\boldsymbol{x}) = \sum_{i \in \mathcal{L}} \sum_{q \in \mathcal{X}_i} x_{qi}^{(k)} - K^{(k)}$, where $K^{(k)}$ is the allowed reuse factor on PRB $k$) or that resource usage must comply with the used technology, e.g., that PRBs must be used on adjacent frequencies for Single-Channel Frequency Division Multiplex (SC-FDM) transmissions.

All nodes are assumed to have a single antenna. Attenuation of the wireless channel between transmitter of link $j$ and receiver of link $i$ on PRB $k$ is captured by the scalar channel coefficient $h_{ij}^{(k)}$, which incorporates the effect of distance dependent path-loss, shadowing and multi-path effects. While drawn randomly according to a given distribution, we assume that $h_{ij}^{(k)}$ remains constant during our optimization.[2] Further, the receiver of link $i$ has a specific noise temperature $\sigma_i^{(k)}$ on PRB $k$. Both, channel and noise value can be equal over different PRBs, e.g., when they reside on the same frequency channel. When all links transmit with a given power on PRB $k$, each receiver will experience an SINR according to

$$\Gamma_i^{(k)}(\boldsymbol{p}) = \frac{h_{ii}^{(k)} p_i^{(k)}}{\sum_{j \neq i} h_{ij}^{(k)} p_j^{(k)} + \sigma_i^{(k)}}. \tag{1}$$

An MCS choice $q_i \in \mathcal{X}_i$ is associated with a minimum SINR requirement $\overline{\gamma}_{q_i}$, which is again gathered in the vectors $\overline{\boldsymbol{\gamma}}_i = [\overline{\gamma}_{q_1}, \ldots, \overline{\gamma}_{q_{|\mathcal{X}_i|}}]^T$ and $\overline{\boldsymbol{\gamma}} = [\overline{\boldsymbol{\gamma}}_1^T, \ldots, \overline{\boldsymbol{\gamma}}_L^T]^T$, respectively. Without loss of generality, we assume that the elements of $\overline{\boldsymbol{\gamma}}_i$ are sorted with increasing value. A transmission on PRB $k$ with MCS $q_i$ yields a data rate of $d_{q_i}$ if $\Gamma_i^{(k)}(\boldsymbol{p}) \geq \overline{\gamma}_{q_i}$ and zero rate otherwise. As before, the values of $d_{q_i}$ are captured by vectors $\boldsymbol{d}_i = [d_{1i}, \ldots, d_{|\mathcal{X}_i|i}]^T$, $\boldsymbol{d} = [\boldsymbol{d}_1^T, \ldots, \boldsymbol{d}_L^T]^T$.

Finally, assume that communication quality is measured by a network utility function $U_i(r_i) : \mathbb{R}_+ \mapsto \mathbb{R}$, which is

[2]Note that we do investigate the impact of channel variations with simulations in Section V.

a function that reflects how desirable a certain instantaneous rate $r_i$ is for communication. The rate reflects the aggregate rate over all PRBs, which are denoted by $r_i^{(k)}\ \forall i \in \mathcal{L}, k \in \mathcal{R}$ and are again grouped according to $\boldsymbol{r}_i = [r_i^{(1)}, \ldots, r_i^{(|\mathcal{R}|)}]^T$, $\boldsymbol{r} = [\boldsymbol{r}_1^T, \ldots, \boldsymbol{r}_{|\mathcal{L}|}^T]^T$. To ensure that the quality of certain links is within the bounds required by the operator, a set of constraints $\boldsymbol{h}(\boldsymbol{r}) \leq \boldsymbol{0}$ is used, which for example can reflect minimum rate constraints if it contains elements $h_i(\boldsymbol{r}) = r_{\min} - r_i$ for minimum rate $r_{\min}$, respectively.

### B. PROBLEM FORMULATION

Using the introduced system model, a general utility maximization problem can be formulated as follows:

$$\max_{\boldsymbol{r},\boldsymbol{x},\boldsymbol{p},\boldsymbol{\gamma}} \sum_{i\in\mathcal{L}} U_i(r_i) \tag{2a}$$

$$\text{s.t. } \boldsymbol{h}(\boldsymbol{r}) \leq \boldsymbol{0} \tag{2b}$$

$$0 \leq r_i \leq \sum_{k\in\mathcal{R}} r_i^{(k)} \tag{2c}$$

$$r_i^{(k)} \leq \boldsymbol{d}_i^T \boldsymbol{x}_i^{(k)} \quad \forall i,k \tag{2d}$$

$$\sum_{q\in\mathcal{X}_i} x_{qi}^{(k)} \leq \mathbb{1}\{k \in \mathcal{R}_i\} \quad \forall i,k \tag{2e}$$

$$\boldsymbol{g}(\boldsymbol{x}) \leq \boldsymbol{0} \tag{2f}$$

$$x_{qi}^{(k)} \in \{0,1\} \forall i,q,k \tag{2g}$$

$$\overline{\boldsymbol{\gamma}}_i^T \boldsymbol{x}_i^{(k)} \leq \gamma_i^{(k)} \quad \forall i,k \tag{2h}$$

$$\gamma_i^{(k)} \left( \sum\nolimits_{j\neq i} \frac{h_{ij}^{(k)}}{h_{ii}^{(k)}} p_j^{(k)} + \frac{\sigma_i^{(k)}}{h_{ii}^{(k)}} \right) \leq p_i^{(k)} \quad \forall i,k \tag{2i}$$

$$\boldsymbol{p}_i \leq \overline{\boldsymbol{p}}_i \quad \forall i \tag{2j}$$

The intuition of this optimization problem is as follows: The utility (2a) to be maximized evaluates the quality of the current network state as aggregation of all per-link utilities. Constraint (2b) is a vector of rate constraints, while (2c) ensures that the evaluated rate does not exceed the actually accumulated one. Both together define an upper Medium Access Control (MAC) layer perspective on the problem, as there is no information on the underlying MAC mechanisms, nor on the actually transported commodities.

In constraints (2d)-(2g), MCSs are set on each PRB. Constraint (2d) guarantees that on each PRB, the assumed rate does not exceed that of the chosen MCS. Constraint (2e) restricts PRB use to the allowed set $\mathcal{R}_i$ and ensures that if the PRB may be used, at most one MCS is set. Constraint (2f) enforces the scheduling constraints and (2g) is an integer constraint for all $x_{qi}^{(k)}$. The four constraints together form a resource allocation perspective, where the rate values $d_i^{(k)}$ act as interface towards the upper layer MAC perspective.

Finally, equations (2h)-(2j) define the actual SINR targets, interference and power constraints on all PRBs. In particular, (2h) ensures that the SINR target $\gamma_i^{(k)}$ satisfies that of the chosen MCS on each PRB, while (2i) is a reformulation of the SINR constraint $\Gamma_i^{(k)}(\boldsymbol{p}) \geq \gamma_i^{(k)}$. Here, variable $\boldsymbol{x}_i^{(k)}$ serves as an interface to the resource allocation part.

It can be seen, and is also indicated by the dashed lines between equations, that the considered problem combines the three aspects of interference management, resource allocation and network utility maximization. Because the utility function is not clearly defined here, the resulting problem can assume a variety of properties only from changing the used utility, rate and scheduling constraints. In this general form, it can be shown to be non-deterministic, polynomial time (NP) complete [26]. However, NP completeness does not come from the undetermined properties of the utility or constraint vectors - as we can show, even for seemingly simple problem instances the problem remains complex:

*Proposition 1* (*NP-Compeleteness for Symmetric, Non-Negative and Increasing Utilities*): Let the utilities be symmetric, non-negative and increasing, such that $U_i(r_i) = U(r_i)\ \forall i$ and $U(0) = 0$, $\partial U(r_i)/\partial r_i > 0\ \forall r_i \geq 0$. Then for any such utility the Problem (2) is NP-complete.

*Proof:* Under the given assumptions, we can reduce the problem to the Reuse Maximization Problem (RMP), which is written as $\max_{\boldsymbol{x},\boldsymbol{p},\boldsymbol{\gamma}} \sum_{i\in\mathcal{L}} x_i$ s.t. (2g)-(2j) with $|\mathcal{R}| = 1$, $|\mathcal{X}_i| = 1$ and which we investigated and showed to be NP-complete in [5], [26]. Consider the special case of $|\mathcal{R}| = 1$, $|\mathcal{X}_i| = 1\ \forall i$ and $\boldsymbol{d}_i = d\ \forall i$, i.e., there is a single PRB and a single MCS available for every link leading to a particular rate $d$, and let the constraint vectors $\boldsymbol{h}(\boldsymbol{r})$, $\boldsymbol{g}(\boldsymbol{x})$ be empty. In this case, it can be seen that the optimal choice of $r_i$ is $r_i = d \cdot x_i$. Because in this case $U(r_i) = U(d \cdot x_i) = U(d)x_i$, problem (2) then reduces to $\max_{\boldsymbol{x},\boldsymbol{p},\boldsymbol{\gamma}} U(d) \sum_{i\in\mathcal{L}} x_i$ s.t. (2g)-(2j) and is equivalent to the RMP. As we can construct such an equivalent problem for any instance of RMP, Problem (2) can be reduced to it and NP-completeness transfers. ■

Note that the conditions given in Proposition 1 apply to some well-known utilities, most prominently to sum-rate ($U(r_i) = r_i$) and proportional-fair rate ($U(r_i) = \log(r_i)$) maximization without any scheduling constraints or rate guarantees. We can thus not expect to solve even these simpler problems optimally and efficiently at the same time, although they have a well-defined utility and no complicating constraints. On the other hand, from a purely technical perspective the efficient, optimal solution is not the only property of interest. Of same or even more importance is well-definedness, i.e., whatever approach we choose to solve the problem should allow a well-defined performance independent of whether it achieves optimality or not. Further, the signaling overhead should be bounded to keep the system efficient and ideally, the same system would allow optimization to different performance metrics, enabling the operators to tune their network as they see fit.

Turning back to Problem (2), in the given formulation, constraint (2i) renders the problem non-convex. However, it is known that constraints (2h)-(2j) can be made convex with a logarithmic transformation [28]–[30], by reformulating $\gamma_i^{(k)} := e^{\tilde{\gamma}_i^{(k)}}$ and $p_i^{(k)} := e^{\tilde{p}_i^{(k)}}$, and using $\tilde{\gamma}_i^{(k)}$ and $\tilde{p}_i^{(k)}$

as variables, respectively. Additionally, we define $\gamma_{\boldsymbol{x}_i}^{(k)} := \overline{\boldsymbol{\gamma}}_i^T \boldsymbol{x}_i^{(k)}$, $\tilde{\gamma}_{\boldsymbol{x}_i}^{(k)} := \log(\gamma_{\boldsymbol{x}_i}^{(k)})$ to be the linear and logarithmically transformed SINR constraint chosen by $\boldsymbol{x}_i$, where for consistency we use $\log(0) := -\infty$ to denote an unbounded negative value. After this transformation, constraints (2i)-(2j) take the form of

$$\tilde{\gamma}_{\boldsymbol{x}_i}^{(k)} \leq \tilde{\gamma}_i^{(k)} \quad \forall i,k \tag{3a}$$

$$e^{\tilde{\gamma}_i^{(k)}} \left( \sum\nolimits_{j \neq i} \frac{h_{ij}^{(k)}}{h_{ii}^{(k)}} e^{\tilde{p}_j^{(k)}} + \frac{\sigma_i^{(k)}}{h_{ii}^{(k)}} \right) e^{-\tilde{p}_i^{(k)}} \leq 1 \quad \forall i,k \tag{3b}$$

$$\tilde{\boldsymbol{p}}_i \leq \tilde{\bar{\boldsymbol{p}}}_i \quad \forall i. \tag{3c}$$

It can be seen that all three constraints are convex. In particular the left hand side of (3b) can be seen to be the sum of convex functions, hence the constraint is also convex. We thus have successfully convexified the SINR constraints.

## III. APPLICATION OF GBD

In this section the application of the Generalized Benders Decomposition (GBD) to the defined problem will be developed. The original Benders decomposition was proposed by Benders [31] for integer linear problems (ILPs) and extended to solve general mixed integer problems by Geoffrion [32]. A comprehensive introduction is given by Floudas [33], who further defined special cases of the GBD that we make use of.

As we do not consider the GBD as well-known procedure, we give a short comprehensive introduction on the main intuition here that roughly follows those given in [32], [33]. For the mathematically concise development, we refer to [32], [33], respectively. The core idea of a GBD is the notion of *complicating variables*. These are variables which, if kept fixed, render the remaining problem efficiently solvable by allowing the application of known solutions or standard techniques. By solving the problem with fixed complicating variables, an outer approximation with respect to these variables can be generated. In particular, consider the problem[3]

$$\min_{\boldsymbol{x},\boldsymbol{y}} f(\boldsymbol{x},\boldsymbol{y}) \quad \text{s.t. } \boldsymbol{g}(\boldsymbol{x},\boldsymbol{y}) \leq \boldsymbol{0}, \tag{4}$$

where $\boldsymbol{y}$ are complicating variables. Then, this problem can equivalently be written as [32]

$$\min_{\boldsymbol{y}} v(\boldsymbol{y}) \text{ s.t. } \boldsymbol{y} \in \mathcal{Y}, \quad \text{where} \tag{5}$$

$$v(\boldsymbol{y}) = \inf_{\boldsymbol{x}} f(\boldsymbol{x},\boldsymbol{y}) \text{ s.t. } \boldsymbol{g}(\boldsymbol{x},\boldsymbol{y}) \leq \boldsymbol{0} \quad \text{and} \tag{6}$$

$$\mathcal{Y} = \{\boldsymbol{y} | \exists \boldsymbol{x} : \boldsymbol{g}(\boldsymbol{x},\boldsymbol{y}) \leq \boldsymbol{0}\}. \tag{7}$$

In words, $v(\boldsymbol{y})$ is obtained by keeping $\boldsymbol{y}$ fixed and optimizing for $\boldsymbol{x}$, while the optimization in $\boldsymbol{y}$ is done in an outer step. Optimization for $\boldsymbol{x}$ is assumed to be "easy" because it is $\boldsymbol{y}$ that complicates the problem. Problem (5) is referred to as *master problem* and that of optimizing the right hand side of (6) as *primal problem*, while $\mathcal{Y}$ is the set of $\boldsymbol{y}$ for which the primal problem has a solution. Under certain assumptions, the function $v(\boldsymbol{y})$ and set $\mathcal{Y}$ can be approximated using Lagrangian duality. In particular, if $f(\boldsymbol{x},\boldsymbol{y})$ and $\boldsymbol{g}(\boldsymbol{x},\boldsymbol{y})$ are convex in $\boldsymbol{x}$ for fixed $\boldsymbol{y}$, then strong duality holds for the primal problem and, given the Lagrange function $L_P(\boldsymbol{x},\boldsymbol{y},\boldsymbol{\lambda})$ for multipliers $\boldsymbol{\lambda}$, it holds that [33]

$$\begin{aligned} v(\boldsymbol{y}) &= \inf_{\boldsymbol{x}} \sup_{\boldsymbol{\lambda} \geq \boldsymbol{0}} L_P(\boldsymbol{x},\boldsymbol{y},\boldsymbol{\lambda}) = \sup_{\boldsymbol{\lambda} \geq \boldsymbol{0}} \inf_{\boldsymbol{x}} L_P(\boldsymbol{x},\boldsymbol{y},\boldsymbol{\lambda}) \\ &\geq \inf_{\boldsymbol{x}} L_P(\boldsymbol{x},\boldsymbol{y},\boldsymbol{\lambda}_k) \ \ \forall \boldsymbol{\lambda}_k \geq \boldsymbol{0}. \end{aligned} \tag{8}$$

According to the last line, for fixed $\boldsymbol{\lambda} := \boldsymbol{\lambda}_k$, the function $\zeta_k(\boldsymbol{y}) = \inf_{\boldsymbol{x}} L_P(\boldsymbol{x},\boldsymbol{y},\boldsymbol{\lambda}_k)$ can be interpreted as supporting function to $v(\boldsymbol{y})$, i.e., $v(\boldsymbol{y}) \geq \zeta_k(\boldsymbol{y})$ and $v(\boldsymbol{y}') = \zeta_k(\boldsymbol{y}')$ for a specific $\boldsymbol{y}'$. As result, $v(\boldsymbol{y})$ can be approximated below by $\hat{v}(\boldsymbol{y}) = \max_k \zeta_k(\boldsymbol{y})$, using a finite number of such $\zeta_k(\boldsymbol{y})$. Similarly, consider the problem

$$\min_{\boldsymbol{x}} 0 \quad \text{s.t. } \boldsymbol{g}(\boldsymbol{x},\boldsymbol{y}) \leq \boldsymbol{0}, \tag{9}$$

which is called *feasibility problem* [32], [33].[4] Given the Lagrangian $L_F(\boldsymbol{x},\boldsymbol{y},\boldsymbol{\lambda})$ associated with this problem, a point $\boldsymbol{y}$ is shown to be in $\mathcal{Y}$ if, and only if [32],

$$\inf_{\boldsymbol{x}} L_F(\boldsymbol{x},\boldsymbol{y},\boldsymbol{\lambda}) \leq 0 \quad \forall \boldsymbol{\lambda} \geq 0. \tag{10}$$

In words, if there exists a single multiplier vector $\boldsymbol{\lambda}$ rendering (10) positive for given $\boldsymbol{y}$, then $\boldsymbol{y} \notin \mathcal{Y}$, and if not, then $\boldsymbol{y} \in \mathcal{Y}$. Similar to the function $v(\boldsymbol{y})$, the set $\mathcal{Y}$ can be outer approximated by a number of constraints $\xi_l(\boldsymbol{y}) \leq 0$, where $\xi_l(\boldsymbol{y}) := \inf_{\boldsymbol{x}} L_F(\boldsymbol{x},\boldsymbol{y},\boldsymbol{\lambda}_l)$ for fixed $\boldsymbol{\lambda}_l$, respectively. Both approximations $\zeta_k(\boldsymbol{y})$ and $\xi_l(\boldsymbol{y})$ lead to a *relaxed master problem* of the form

$$\min_{\mu,\boldsymbol{y}} \mu \quad \text{s.t. } \mu \geq \zeta_k(\boldsymbol{y}) \ \ \forall k, \ \ \xi_l(\boldsymbol{y}) \leq 0 \ \ \forall l, \tag{11}$$

where the constraints $\mu \geq \zeta_k(\boldsymbol{y})$ $\forall k$ realize the function $\hat{v}(\boldsymbol{y}) = \max_k \zeta_k(\boldsymbol{y})$ and the constraints $\xi_l(\boldsymbol{y}) \leq 0$ approximate $\mathcal{Y}$, respectively.

The rough flow of the GBD algorithm now follows by iteratively re-fining the set of $\zeta_k(\boldsymbol{y})$ and $\xi_l(\boldsymbol{y})$ [32], [33]: (0) Start with an approximation of $v(\boldsymbol{y})$ and $\mathcal{Y}$. (1) Solve the relaxed master problem, yielding an outcome $\boldsymbol{y}_k$. (2) If the primal problem is feasible, identify new function $\zeta_k(\boldsymbol{y})$ and add constraint $\mu \geq \zeta_k(\boldsymbol{y})$. This re-fines the approximation of $v(\boldsymbol{y})$. (3) If it is infeasible, identify $\boldsymbol{\lambda}_l$ such that $\xi_l(\boldsymbol{y}_k) > 0$ and add constraint $\xi_l(\boldsymbol{y}) \leq 0$. This re-fines the approximation of $\mathcal{Y}$. (4) If optimality criterion is not met, go to (1).

The multipliers $\boldsymbol{\lambda}_l$ in step (3) can be identified as Lagrange multipliers associated with the solution to particular feasibility problems, as is summarized in [33], respectively. The given algorithm describes an iterative solution that relies on a consecutive outer approximation of the problem space. That is, the master problem starts with a coarse approximation of its problem space and optimizing function and with each iteration a new constraint is added that refines the problem,

[3] Note that we re-use variables here due to the standardized formulation of optimization problems [32], [33]. These have nothing to do with the variables for the utility function given in the previous and following sections.

[4] Because the objective function is constant, any feasible point is also optimal, so the problem is that of finding a random feasible point.

until it is accurate enough to allow an optimal solution (or in general, until a convergence criterion such as a maximum error bound is satisfied). A key property is finite convergence, which guarantees that the refinement terminates within a finite number of steps. This holds under certain conditions, e.g., if the master problem is purely integer [32].

### A. PRIMAL AND FEASIBILITY PROBLEM

We will now generate the primal and feasibility problem of the GBD. We choose $\boldsymbol{x}$ and $\boldsymbol{r}$ as complicating variables, such that they are kept fixed in the primal and feasibility problem. As result, all constraints that only contain complicating variables can be neglected. In particular, the constraints $\boldsymbol{h}(\boldsymbol{r})$ and $\boldsymbol{g}(\boldsymbol{x})$ contain only complicating variables and hence play no role for the primal and feasibility problem. The primal problem can be formulated as

$$\text{(P)} \quad \max_{\tilde{\boldsymbol{p}},\tilde{\boldsymbol{\gamma}}} \sum_{i\in\mathcal{L}} U_i(r_i) \tag{12a}$$

$$\text{s.t. } \tilde{\gamma}_{\boldsymbol{x}_i}^{(k)} \le \tilde{\gamma}_i^{(k)} \quad \forall i,k \tag{12b}$$

$$e^{\tilde{\gamma}_i^{(k)}} \left( \sum\nolimits_{j\neq i} \frac{h_{ij}^{(k)}}{h_{ii}^{(k)}} e^{\tilde{p}_j^{(k)}} + \frac{\sigma_i^{(k)}}{h_{ii}^{(k)}} \right) e^{-\tilde{p}_i^{(k)}} \le 1 \quad \forall i,k \tag{12c}$$

$$\tilde{\boldsymbol{p}}_i \le \tilde{\bar{\boldsymbol{p}}}_i \quad \forall i. \tag{12d}$$

If (P) is found to be infeasible due to the choice of $\boldsymbol{x}$, a feasibility problem is solved, which is of the form [33, Ch. 6.3.3.1]:

$$\text{(F)} \quad \min_{z,\tilde{\boldsymbol{p}},\tilde{\boldsymbol{\gamma}}} \sqrt[p]{\sum_{i\in\mathcal{L}}\sum_{k\in\mathcal{R}} \left(z_i^{(k)}\right)^p} \tag{13a}$$

$$\text{s.t. } z_i^{(k)} \ge 0 \ \ \forall i,k \tag{13b}$$

$$\tilde{\gamma}_{\boldsymbol{x}_i}^{(k)} \le \tilde{\gamma}_i^{(k)} \ \ \forall i,k \tag{13c}$$

$$e^{\tilde{\gamma}_i^{(k)}} \left( \sum\nolimits_{j\neq i} \frac{h_{ij}^{(k)}}{h_{ii}^{(k)}} e^{\tilde{p}_j^{(k)}} + \frac{\sigma_i^{(k)}}{h_{ii}^{(k)}} \right) e^{-\tilde{p}_i^{(k)}} - 1 \le z_i^{(k)} \tag{13d}$$

$$\tilde{\boldsymbol{p}}_i \le \tilde{\bar{\boldsymbol{p}}}_i \ \ \forall i. \tag{13e}$$

The feasibility problem aims at minimizing the slack variables $z_i^{(k)}$ on equation (13d) with respect to an $\ell^p$ norm for $p \in \mathbb{N}_+$, $p \ge 1$, under the constraint that $z_i^{(k)} \ge 0$. As is summarized in [33], the optimal Lagrange multipliers of (F) satisfy $\xi_l(\boldsymbol{y}) > 0$ whenever (P) is infeasible. On the other hand, the optimal value of (F) is zero if and only if (P) is feasible.

We can now compare the two problems (P) and (F) and find that (P) can be solved by (F): As the utility of (P) is constant, any feasible point is in fact also optimal. However, if a feasible point exist, it is found by the feasibility problem. As result, it is sufficient to optimize (F).

### B. INVESTIGATION OF THE FEASIBILITY PROBLEM

As can be seen from (13c) and (13d) that, without loss of generality, $\tilde{\gamma}_i^{(k)} := \tilde{\gamma}_{\boldsymbol{x}_i}^{(k)}$ is an optimal variable choice, because it is the feasible value of $\tilde{\gamma}_i^{(k)}$ that allows the smallest value of $z_i^{(k)}$. This choice corresponds to setting the SINR constraint to that imposed by the fixed MCS variable $\boldsymbol{x}_i^{(k)}$. Using this, (13d) can be reformulated into

$$\frac{e^{\tilde{\gamma}_{\boldsymbol{x}_i}^{(k)}}}{1+z_i^{(k)}} \left( \sum_{j\neq i} \frac{h_{ij}^{(k)}}{h_{ii}^{(k)}} e^{\tilde{p}_j^{(k)}} + \frac{\sigma_i^{(k)}}{h_{ii}^{(k)}} \right) - e^{\tilde{p}_i^{(k)}} \le 0. \tag{14}$$

We now define the values $\gamma_i^{(k)'} := e^{\tilde{\gamma}_i^{(k)'}} = e^{\tilde{\gamma}_{\boldsymbol{x}_i}^{(k)}}/(1+z_i^{(k)})$, which can be interpreted as an achieved SINR, as the term may take any value smaller than the actual SINR. Reverting the relationship yields $z_i^{(k)} = e^{\tilde{\gamma}_{\boldsymbol{x}_i}^{(k)} - \tilde{\gamma}_i^{(k)'}} - 1$. By plugging the relations into (F), a problem equivalent to (F) can stated as:

$$\min_{\tilde{\boldsymbol{p}},\tilde{\boldsymbol{\gamma}}'} \sum_{i\in\mathcal{L}}\sum_{k\in\mathcal{R}} \left( e^{\tilde{\gamma}_{\boldsymbol{x}_i}^{(k)} - \tilde{\gamma}_i^{(k)'}} - 1 \right)^p$$

$$\text{s.t. } \tilde{\gamma}_i^{(k)'} \le \tilde{\gamma}_{\boldsymbol{x}_i}^{(k)} \ \ \forall i,k \tag{15}$$

$$e^{\tilde{\gamma}_i^{(k)'}} \left( \sum\nolimits_{j\neq i} \frac{h_{ij}^{(k)}}{h_{ii}^{(k)}} e^{\tilde{p}_j^{(k)}} + \frac{\sigma_i^{(k)}}{h_{ii}^{(k)}} \right) - e^{\tilde{p}_i^{(k)}} \le 0 \ \ \forall i,k \tag{16}$$

$$e^{\tilde{p}_i^{(k)}} \le \bar{p}_i^{(k)} \ \ \forall i,k. \tag{17}$$

In words, the feasibility problem is that of minimizing a polynomial of factors $\gamma_{\boldsymbol{x}_i}^{(k)}/\gamma_i^{(k)'}$, under the constraints that the variables $\gamma_i^{(k)'}$ exceed neither the achieved SINR (equation (16)), nor the targets $\gamma_{\boldsymbol{x}_i}^{(k)}$ (equation (15)). The stated problem is convex on continuous problem space and satisfies Slaters' condition. Hence, it has either one unique local optimum that is also globally optimal or several local optima that all are globally optimal. For any local optimum, the Karush-Kuhn-Tucker (KKT) conditions are necessary and sufficient, hence they can serve to identify optimal points. The associated Lagrange function is:

$$\begin{aligned} L = \sum_{i\in\mathcal{L}}\sum_{k\in\mathcal{R}} \Bigg[ & \left( e^{\tilde{\gamma}_{\boldsymbol{x}_i}^{(k)} - \tilde{\gamma}_i^{(k)'}} - 1 \right)^p \\ & + \mu_i^{(k)} \left[ \tilde{\gamma}_i^{(k)'} - \tilde{\gamma}_{\boldsymbol{x}_i}^{(k)} \right] + \nu_i^{(k)} \left[ e^{\tilde{p}_i^{(k)}} - \bar{p}_i^{(k)} \right] \\ & + \eta_i^{(k)} \left[ e^{\tilde{\gamma}_i^{(k)'}} \left( \sum_{j\neq i} \frac{h_{ij}^{(k)}}{h_{ii}^{(k)}} e^{\tilde{p}_j} + \frac{\sigma_i^{(k)}}{h_{ii}^{(k)}} \right) - e^{\tilde{p}_i^{(k)}} \right] \Bigg], \end{aligned} \tag{18}$$

where $\mu_i^{(k)} \ge 0$, $\eta_i^{(k)} \ge 0$ and $\nu_i^{(k)} \ge 0$ are multipliers. As the defined problem is convex, the optimal solution can be found by solving $\min_{\tilde{\boldsymbol{p}},\tilde{\boldsymbol{\gamma}}'} \max_{\boldsymbol{\mu},\boldsymbol{\eta},\boldsymbol{\nu}} L(\tilde{\boldsymbol{p}}, \tilde{\boldsymbol{\gamma}}', \boldsymbol{\mu}, \boldsymbol{\eta}, \boldsymbol{\nu})$. That is, $\tilde{\boldsymbol{p}}$ and $\tilde{\boldsymbol{\gamma}}'$ should be chosen to minimize $L$, whereas $\boldsymbol{\mu}$, $\boldsymbol{\eta}$ and $\boldsymbol{\nu}$ should be chosen to maximize it. The KKT conditions can be derived by setting $\partial L/\partial \tilde{\gamma}_i^{(k)'} = 0$ and $\partial L/\partial \tilde{p}_i^{(k)} = 0$. The derivatives of the Lagrange function $L$ with respect to $\tilde{\gamma}_i^{(k)'}$ and $\tilde{p}_i^{(k)}$ are:

$$\begin{aligned} \partial L/\partial \tilde{\gamma}_i^{(k)'} = & -p e^{\tilde{\gamma}_{\boldsymbol{x}_i}^{(k)} - \tilde{\gamma}_i^{(k)'}} \left( e^{\tilde{\gamma}_{\boldsymbol{x}_i}^{(k)} - \tilde{\gamma}_i^{(k)'}} - 1 \right)^{p-1} \\ & + \eta_i^{(k)} e^{\tilde{\gamma}_i^{(k)'}} \left( \sum_{j\neq i} \frac{h_{ij}^{(k)}}{h_{ii}^{(k)}} e^{\tilde{p}_j} + \frac{\sigma_i^{(k)}}{h_{ii}^{(k)}} \right) + \mu_i^{(k)} \end{aligned} \tag{19}$$

$$\partial L/\partial \tilde{p}_i^{(k)} = e^{\tilde{p}_i^{(k)}} \left[ \sum_{j \neq i} e^{\tilde{\gamma}_j^{(k)'}} \frac{h_{ji}}{h_{jj}} \eta_j^{(k)} - \eta_i^{(k)} + \nu_i^{(k)} \right]. \quad (20)$$

The corresponding complementary slackness conditions are:

$$\eta_i^{(k)} \left[ e^{\tilde{\gamma}_i^{(k)'}} \left( \sum_{j \neq i} \frac{h_{ij}^{(k)}}{h_{ii}^{(k)}} e^{\tilde{p}_j^{(k)}} + \frac{\sigma_i^{(k)}}{h_{ii}^{(k)}} \right) - e^{\tilde{p}_i^{(k)}} \right] = 0 \ \ \forall i, k$$

$$\nu_i^{(k)} \left[ e^{\tilde{p}_i^{(k)}} - \overline{p}_i^{(k)} \right] = 0; \qquad \mu_i^{(k)} \left[ \tilde{\gamma}_i^{(k)'} - \tilde{\gamma}_{\boldsymbol{x}_i}^{(k)} \right] = 0 \ \ \forall i, k.$$

Now some properties of optimal solutions can be observed:

*Proposition 2:* There always is an optimal point such that $\gamma_i^{(k)'} = \min\{\Gamma_i^{(k)}(\boldsymbol{p}), \gamma_{\boldsymbol{x}_i}^{(k)}\}$.

*Proof:* Observe that if $\gamma_i^{(k)'} = \gamma_{\boldsymbol{x}_i}^{(k)}$, constraint (15) is tight and if $\gamma_i^{(k)'} = \Gamma_i^{(k)}(\boldsymbol{p})$, constraint (16) is. Assume that $\gamma_i^{(k)'} < \min\{\Gamma_i^{(k)}(\boldsymbol{p}), \gamma_{\boldsymbol{x}_i}^{(k)}\}$, then due to the complementary slackness conditions, $\eta_i^{(k)} = \mu_i^{(k)} = 0$. Plugging this into (19) leads to $\partial L/\partial \tilde{\gamma}_i^{(k)'} < 0$. Thus, by increasing $\tilde{\gamma}_i^{(k)'}$, a lower value of $L$ can be obtained and the chosen $\gamma_i^{(k)'}$ cannot be optimal. The result is that for the optimal $\tilde{\gamma}_i^{(k)'}$ one of (15), (16) must be tight, leading to the stated observation. ∎

*Proposition 3:* There always exists an optimal point for which $\gamma_i^{(k)'} = \Gamma_i^{(k)}(\boldsymbol{p})\ \forall i$ holds. *Proof:* Again observe that $\gamma_i^{(k)'} = \Gamma_i^{(k)}(\boldsymbol{p})$ corresponds to constraint (16) being tight. Assume that $\gamma_i^{(k)'} < \Gamma_i^{(k)}(\boldsymbol{p})$ at optimality, then due to the complementary slackness conditions, $\eta_i^{(k)} = 0$. As all considered variables are non-negative, plugging this into (20) leads to $\partial L/\partial \tilde{p}_i^{(k)} \geq 0$, with equality if, and only if $\boldsymbol{\eta} = \boldsymbol{0}$ and $\nu_i^{(k)} = 0$. Due to the complementary slackness conditions, the case of all multipliers being zero can be optimal only when all links fully achieve the SINR targets $\gamma_{\boldsymbol{x}_i}^{(k)}$, i.e., when (P) is feasible. In this case any feasible power vector is an optimal point, so there can be multiple optima. If $\partial L/\partial \tilde{p}_i^{(k)} = 0$ holds, the value of $\tilde{p}_i^{(k)}$ may be decreased until $\gamma_i^{(k)'} = \Gamma_i^{(k)}(\boldsymbol{p})$ without loosing optimality. Otherwise, $\partial L/\partial \tilde{p}_i^{(k)} > 0$, so by decreasing $\tilde{p}_i^{(k)}$ the value of $L$ will definitely be decreased, leading to a contradiction on the optimality assumption. ∎

*Proposition 4:* For at least one optimal point,

$$p_i^{(k)} = \min \left\{ \gamma_{\boldsymbol{x}_i}^{(k)} \left( \sum_{j \neq i} \frac{h_{ij}^{(k)}}{h_{ii}^{(k)}} p_j^{(k)} + \frac{\sigma_i^{(k)}}{h_{ii}^{(k)}} \right), \overline{p}_i^{(k)} \right\} \ \ \forall i \quad (21)$$

holds. *Proof:*

The combination of Proposition 2 and 3 lead to the corollary that there is an optimal point such that $\Gamma_i^{(k)}(\boldsymbol{p}) = \gamma_i^{(k)'} \leq \gamma_{\boldsymbol{x}_i}^{(k)}\ \forall i$. Using the expression for SINR, this can be reformulated into

$$p_i^{(k)} \leq \gamma_{\boldsymbol{x}_i}^{(k)} \left( \sum_{j \neq i} \frac{h_{ij}^{(k)}}{h_{ii}^{(k)}} p_j^{(k)} + \frac{\sigma_i^{(k)}}{h_{ii}^{(k)}} \right), \quad (22)$$

which holds with equality if, and only if, $\gamma_i^{(k)'} = \gamma_{\boldsymbol{x}_i}^{(k)}$. Equation (21) thus corresponds to the claim that if $\gamma_i^{(k)'} < \gamma_{\boldsymbol{x}_i}^{(k)}$, then $p_i^{(k)} = \overline{p}_i^{(k)}$ must hold. To prove this, a perturbation analysis is done: Assume that $\gamma_i^{(k)'} < \gamma_{\boldsymbol{x}_i}^{(k)}$ and $p_i^{(k)} < \overline{p}_i^{(k)}$, which induces $\mu_i^{(k)} = 0$ and $\nu_i^{(k)} = 0$, i.e., no constraint is active and the optimal values $\gamma_i^{(k)'}$ and $p_i^{(k)}$ are in the relative interior of their feasible domains. Because of this, the value of $\gamma_{\boldsymbol{x}_i}^{(k)}$ can be unilaterally altered into any value $\gamma_{\boldsymbol{x}_i}^{(k)'}$, $\gamma_i^{(k)'} < \gamma_{\boldsymbol{x}_i}^{(k)'} < \gamma_{\boldsymbol{x}_i}^{(k)}$, while keeping $\gamma_{\boldsymbol{x}_j}^{(k)}$ with $j \neq i$ constant. Now the original problem using $\gamma_{\boldsymbol{x}_i}^{(k)}$ can be interpreted as relaxation of the perturbed problem with $\gamma_{\boldsymbol{x}_i}^{(k)'}$. It is known that if the solution of a relaxed problem lies in the non-relaxed optimization domain, it is also optimal for the non-relaxed problem [33]. So as the optimal values of $p_i^{(k)}$, $\gamma_i^{(k)'}$ are within the perturbed optimization domain by design, they must remain optimal throughout the perturbation process. However, by demanding $\partial L/\partial \tilde{\gamma}_i^{(k)'} = \partial L/\partial \tilde{p}_i^{(k)} = 0$, considering that $\mu_i^{(k)} = \nu_i^{(k)} = 0\ \forall i, k$ still holds, reformulating (19), (20) and combining the results, it can be deduced that at any optimal point,

$$\eta_i^{(k)} = \sum_{j \neq i} \gamma_j^{(k)'} \frac{h_{ji}^{(k)}}{h_{jj}^{(k)}} \eta_j^{(k)}; \quad \eta_i^{(k)} = \frac{p \gamma_{\boldsymbol{x}_i}^{(k)} \left( \frac{\gamma_{\boldsymbol{x}_i}^{(k)'}}{\gamma_i^{(k)'}} - 1 \right)^{p-1}}{(\gamma_i^{(k)'})^2 I_i^{(k)}(\boldsymbol{p})}; \quad (23)$$

where $I_i^{(k)}(\boldsymbol{p}) = \sum_{j \neq i} \frac{h_{ji}^{(k)}}{h_{ii}^{(k)}} p_j^{(k)} + \frac{\sigma_i^{(k)}}{h_{ii}^{(k)}}$. It can be seen that in the right expression, $\eta_i^{(k)}$ depends on $\gamma_{\boldsymbol{x}_i}^{(k)'}$ but is independent of $\gamma_{\boldsymbol{x}_j}^{(k)}, j \neq i$. In the left expression $\eta_i^{(k)}$ depends on all $\gamma_{\boldsymbol{x}_j}^{(k)}$ because the optimal multipliers $\eta_j^{(k)}$ do, respectively, but is independent of $\gamma_{\boldsymbol{x}_i}^{(k)'}$. Any unilateral change of $\gamma_{\boldsymbol{x}_i}^{(k)'}$ cannot satisfy both expressions anymore, because it would change the optimal $\eta_i^{(k)}$, while $\eta_j^{(k)}$ would have to remain constant. So optimal points of the original problem cannot remain optimal after perturbation. This forms a contradiction to the assumption that $\gamma_i^{(k)'}$, $p_i^{(k)}$ are in the relative interior of the optimization domain, for which they would have to remain optimal. As conclusion, $\gamma_i^{(k)'} < \gamma_{\boldsymbol{x}_i}^{(k)}$ and $p_i^{(k)} < \overline{p}_i^{(k)}$ cannot hold at the same time. Taking this result, the conclusion is that if $\gamma_i^{(k)'} = \Gamma_i^{(k)}(\boldsymbol{p}) < \gamma_{\boldsymbol{x}_i}^{(k)}$, then $p_i^{(k)} = \overline{p}_i^{(k)}$ must hold and vice versa, leading to equation (21). ∎

The result of Proposition 4 is important, as it relates the RMP to a set of well-known power control algorithms. The power-constrained Foschini-Miljanic PCA (FM-PCA) [34] iteratively adapts powers exactly according to the rule

$$p_i^{(k)}[t+1] = \min \left\{ \gamma_{\boldsymbol{x}_i}^{(k)} \left( \sum_{j \neq i} \frac{h_{ij}^{(k)}}{h_{ii}^{(k)}} p_j^{(k)}[t] + \frac{\sigma_i^{(k)}}{h_{ii}^{(k)}} \right), \overline{p}_i^{(k)} \right\}. \quad (24)$$

It is known to always converge to a unique point, at which (21) holds. The power control algorithm (PCA) can be implemented in a distributed fashion, where each transmitter and receiver optimize solely themselves but do not coordinate

with other links. Also, it does not require any explicit information on channel gains but can be implemented using SINR values, because the left part of the update rule can be interpreted as [35]:

$$\gamma_{\boldsymbol{x}_i}^{(k)}\left(\frac{\sum_{j\neq i}h_{ij}^{(k)}p_j^{(k)}[t]+\sigma_i^{(k)}}{h_{ii}^{(k)}p_i^{(k)}[t]}\right)p_i^{(k)}[t]=\frac{\gamma_{\boldsymbol{x}_i}^{(k)}}{\Gamma_i^{(k)}(\boldsymbol{p}[t])}p_i^{(k)}[t]. \tag{25}$$

The PCA is known to converge towards its solution with at least linear rate. Typically, convergence can be claimed after 6-10 iterations, where one iteration comprises one transmission and one SINR feedback. The algorithm has been further re-fined for a variety of use-cases, including the use of safety margins on the SINR target [35], asynchronous operation [36] and discrete power levels [37].

The conclusion of Proposition 4 is that Foschini-Miljanic type PCAs can be used to determine the optimal solution of the feasibility problem. By letting the algorithm run for a sufficient amount of iterations and then setting $\gamma_i^{(k)'} = \Gamma_i^{(k)}(\boldsymbol{p})$, the optimal value of $\gamma_i^{(k)'}$ can be found.

### C. THE MASTER PROBLEM

After adapting the feasibility problem, the master problem needs to be derived. In particular, constraints must be added to it from each instance of (P) and (F). We start with constraints of (F), which generate a bound of the form $\xi_l(\boldsymbol{x},\boldsymbol{r}) \leq 0$. Let $\boldsymbol{x}_l$, $\boldsymbol{r}_l$ be the current choice of complicating variables. We need to identify the arguments of $\arg\min_{\tilde{\boldsymbol{p}},\tilde{\boldsymbol{\gamma}}}\max_{\tilde{\boldsymbol{\gamma}},\boldsymbol{\tau},\boldsymbol{\eta},\boldsymbol{\nu}}\overline{L}_F(\boldsymbol{x}_l,\boldsymbol{r}_l,\tilde{\boldsymbol{p}},\tilde{\boldsymbol{\gamma}},\boldsymbol{\tau},\boldsymbol{\eta},\boldsymbol{\nu})$ to generate $\xi_l(\boldsymbol{x},\boldsymbol{r})$ [32]. By considering the formulation (13a)-(13c), the Lagrangian function corresponding to (F) takes the form of:

$$\begin{aligned}L_F = \|z\|_p &+ \sum_{i\in\mathcal{L}}\sum_{k\in\mathcal{R}}\left[\tau_i^{(k)}\left[\tilde{\gamma}_{\boldsymbol{x}_i}^{(k)}-\tilde{\gamma}_i^{(k)}\right]\right.\\ &+\nu_i^{(k)}\left[e^{\tilde{p}_i^{(k)}}-\overline{p}_i^{(k)}\right]-\sum_{i\in\mathcal{L}}\mu_i^{(k)}z_i^{(k)}+\\ &\left.\eta_i^{(k)}\left[e^{\tilde{\gamma}_i^{(k)}}\left(\sum_{j\neq i}\frac{h_{ij}^{(k)}}{h_{ii}^{(k)}}e^{\tilde{p}_j^{(k)}}+\frac{\sigma_i^{(k)}}{h_{ii}^{(k)}}\right)e^{-\tilde{p}_i^{(k)}}-1-z_i^{(k)}\right]\right].\end{aligned} \tag{26}$$

where $\tau_i^{(k)} \geq 0$, $\eta_i^{(k)} \geq 0$, $\nu_i^{(k)} \geq 0$ and $\mu_i^{(k)} \geq 0$ are multipliers. Defining $\overline{L}_F$ to be $L_F \mid_{z=0}$, $\xi_l(\boldsymbol{x},\boldsymbol{r}) = \inf_{\tilde{\boldsymbol{p}},\tilde{\boldsymbol{\gamma}}}\overline{L}_F(\boldsymbol{x},\boldsymbol{r},\tilde{\boldsymbol{p}},\tilde{\boldsymbol{\gamma}},\boldsymbol{\tau}_l,\boldsymbol{\eta}_l,\boldsymbol{\nu}_l)$ is given by [32]:

$$\xi_l(\boldsymbol{x},\boldsymbol{r})=\sum_{i\in\mathcal{L}}\sum_{k\in\mathcal{R}}\left[\tau_i^{(k)}\left[\log(\overline{\boldsymbol{\gamma}}_i^T\boldsymbol{x}_i^{(k)})-\tilde{\gamma}_i^{(k)}\right]+\eta_i^{(k)}\left[\frac{\gamma_{\boldsymbol{x}_l,i}^{(k)}}{\Gamma_i^{(k)}(\boldsymbol{p})}-1\right]\right],$$

where the variables $\boldsymbol{\tau}_l$, $\boldsymbol{\eta}_l$ and $\boldsymbol{\nu}_l$ are kept fixed at the optimal values derived from minimizing $L_F$ [33]. It was used that for fixed multipliers, the optimization with respect to $\tilde{\boldsymbol{p}}$ and $\tilde{\boldsymbol{\gamma}}$ is independent of the complicating variables $\boldsymbol{x}$, $\boldsymbol{r}$ and that the optimal values must equal those derived in the instance of (F) [33]. As result, all neglected terms must be zero due to the complementary slackness conditions. It can be seen that $\xi_l(\boldsymbol{x},\boldsymbol{r}) = \xi_l(\boldsymbol{x})$ is in fact independent of $\boldsymbol{r}$. It remains to derive the optimal values of $\tau_i^{(k)}$ and $\eta_i^{(k)}$. Consider the derivatives of the Lagrangian $L_F$,

$$\partial L_F/\partial z_i^{(k)} = \left(\frac{z_i^{(k)}}{\|z\|_p}\right)^{p-1}-\eta_i^{(k)}-\mu_i^{(k)}, \tag{27}$$

$$\partial L_F/\partial\tilde{\gamma}_i^{(k)} = \eta_i^{(k)}e^{\tilde{\gamma}_i^{(k)}}/\Gamma_i^{(k)}(\tilde{\boldsymbol{p}})-\tau_i^{(k)}, \tag{28}$$

and the complementary slackness conditions:

$$\eta_i^{(k)}\left[e^{\tilde{\gamma}_i^{(k)}}/\Gamma_i^{(k)}(\tilde{\boldsymbol{p}})-1-z_i^{(k)}\right]=0;\quad \mu_i^{(k)}z_i^{(k)}=0.$$

*Proposition 5:* The choices of

$$\tau_i^{(k)} := \eta_i^{(k)}\frac{\gamma_{\boldsymbol{x}_l,i}^{(k)}}{\Gamma_i^{(k)}(\boldsymbol{p})};\quad \eta_i^{(k)}=\left(\frac{z_i^{(k)}}{\|z\|_p}\right)^{p-1}$$
$$\text{with } z_i^{(k)} := \left[\frac{\gamma_{\boldsymbol{x}_l,i}^{(k)}}{\Gamma_i^{(k)}(\boldsymbol{p})}-1\right]^+ \forall i,k \tag{29}$$

are optimal multipliers.

*Proof:* Setting $\partial L_F/\partial\tilde{\gamma}_i^{(k)}$ to zero yields $\tau_i^{(k)} := \eta_i^{(k)}\gamma_i^{(k)}/\Gamma_i^{(k)}(\boldsymbol{p}) = \eta_i^{(k)}\gamma_{\boldsymbol{x}_i}^{(k)}/\Gamma_i^{(k)}(\boldsymbol{p})$, where the optimal choice of $\gamma_i^{(k)} := \gamma_{\boldsymbol{x}_i}^{(k)}$ was used. Now, assume that at optimality, $z_i^{(k)} > 0$. From the complementary slackness, this leads to $\mu_i^{(k)} = 0$, to $\eta_i^{(k)} = \left(z_i^{(k)}/\|z\|_p\right)^{p-1}$ from setting $\partial L_F/\partial z_i^{(k)}$ to zero and hence to the stated result by using the optimal value of $z_i^{(k)}$. On the other hand, assume that $z_i^{(k)} = 0$, then $\mu_i^{(k)}+\eta_i^{(k)} = 0$ must hold for $p > 1$, yielding $\tau_i^{(k)} = \eta_i^{(k)} = 0$. A special case is $p = 1$ and $z_i^{(k)} = 0$, in which $\mu_i^{(k)}+\eta_i^{(k)} = 1$ must hold. In this case, for any value of $\mu_i^{(k)} \in [0,1]$ there is a $\eta_i^{(k)} \geq 0$ such that $\partial L_F/\partial z_i^{(k)}$ is zero, rendering both together optimal. Although not unique, the choice $\mu_i^{(k)} = 0$ remains an optimal multiplier here and leads to $\eta_i^{(k)} = 1$ and $\tau_i^{(k)} = \gamma_{\boldsymbol{x}_i}^{(k)}/\Gamma_i^{(k)}(\boldsymbol{p})$, respectively. ∎

This finally yields functions of the form:

$$\xi_l(\boldsymbol{x})=\sum_{i\in\mathcal{L}}\sum_{k\in\mathcal{R}}\left[\tau_{l,i}^{(k)}\left[\log(\overline{\boldsymbol{\gamma}}_i^T\boldsymbol{x}_i^{(k)})-\tilde{\gamma}_{\boldsymbol{x}_l,i}^{(k)}\right]+\eta_{l,i}^{(k)}z_{l,i}^{(k)}\right] \tag{30}$$

where

$$\tau_{l,i}^{(k)} := \left(\frac{z_{l,i}^{(k)}}{\|z_l\|_p}\right)^{p-1}\frac{\gamma_{\boldsymbol{x}_l,i}^{(k)}}{\Gamma_i^{(k)}(\boldsymbol{p}_l)},\ \eta_{l,i}^{(k)}=\left(\frac{z_{l,i}^{(k)}}{\|z\|_p}\right)^{p-1},$$
$$z_{l,i}^{(k)} := \left[\frac{\gamma_{\boldsymbol{x}_l,i}^{(k)}}{\Gamma_i^{(k)}(\boldsymbol{p}_l)}-1\right]^+ \forall i,k.$$

Now consider a feasible primal problem, in which case a constraint $\zeta_k(\boldsymbol{x},\boldsymbol{r})$ is generated from the Lagrange function

of (P). The Lagrange function reads:

$$L_P = \sum_{i\in\mathcal{L}}\left[-U_i(r_i) + \sum_{k\in\mathcal{R}} \tau_i^{(k)}\left[\tilde{\gamma}_{\boldsymbol{x}_i}^{(k)} - \tilde{\gamma}_i^{(k)}\right]\right] + \sum_{i\in\mathcal{L}}\sum_{k\in\mathcal{R}}\left[\eta_i^{(k)}\left[\frac{e^{\tilde{\gamma}_i^{(k)}}}{\Gamma_i^{(k)}(\tilde{\boldsymbol{p}})} - 1\right] + \nu_i^{(k)}\left[e^{\tilde{p}_i^{(k)}} - \overline{p}_i^{(k)}\right]\right].$$

This leads to a constraint function of:

$$\begin{aligned}\zeta(\boldsymbol{x},\boldsymbol{r}) &= \min_{\tilde{\boldsymbol{p}},\tilde{\boldsymbol{\gamma}}} L_P(\boldsymbol{x},\boldsymbol{r},\tilde{\boldsymbol{p}},\tilde{\boldsymbol{\gamma}}) \\ &= -\sum_{i\in\mathcal{L}} U_i(r_i) + \sum_{k\in\mathcal{R}} \tau_i^{(k)}\left[\log(\overline{\boldsymbol{\gamma}}_i^T \boldsymbol{x}_i^{(k)}) - \tilde{\gamma}_{\boldsymbol{x}_l,i}^{(k)}\right],\end{aligned}$$

where the same arguments as for $\xi_l(\boldsymbol{x})$ were used. Again, an optimal value of the multipliers $\tau_i^{(k)}$ must be determined. We have argued already that any feasible point found with the feasibility problem (F) is also optimal to (P). Further, the difference among their Lagrangian functions is $L_F - L_P = \sum_i U_i(r_i)$, which is a constant term for fixed $\boldsymbol{r}$. As result, the KKT and complementary slackness conditions of $L_F$ and $L_P$ are the same, rendering optimal multipliers derived from (F) with $\boldsymbol{z} = \boldsymbol{0}$ also optimal for (P). As we have argued in the context of (F), for $z_i^{(k)} = 0$, any multiplier $\eta_i^{(k)} \in [0,1]$ can be claimed optimal, from which follows that any $\tau_i^{(k)} \in [0, \gamma_{\boldsymbol{x}_i}^{(k)}/\Gamma_i^{(k)}(\boldsymbol{p})]$ is optimal for (P). We choose $\tau_i^{(k)} = 0$ in this context, as it simplifies the form of $\zeta_k(\boldsymbol{x},\boldsymbol{r})$ to:

$$\zeta_k(\boldsymbol{x},\boldsymbol{r}) = -\sum_{i\in\mathcal{L}} U_i(r_i).$$

The obtained master problem in general form is that of [32]:

$$\text{(M)}\quad \min_{\mu,\boldsymbol{x},\boldsymbol{r}} \mu \text{ s.t. } \mu \geq \zeta_k(\boldsymbol{x},\boldsymbol{r}),\quad \text{(2c)-(2g)},\quad \xi_l(\boldsymbol{x}) \leq 0 \;\; \forall l.$$

By using the generated bounds, it can be stated in explicit form as:

$$\begin{aligned}\text{(M)}\quad &\max_{\boldsymbol{x},\boldsymbol{r}} \sum_{i\in\mathcal{L}} U_i(r_i) \\ &\text{s.t. (2c)-(2g)},\quad \sum_{i\in\mathcal{L}}\sum_{k\in\mathcal{R}} \tau_{l,i}^{(k)} \log(\overline{\boldsymbol{\gamma}}_i^T \boldsymbol{x}_i^{(k)}) \leq W_l \forall l, \quad (31)\end{aligned}$$

where $W_l = \boldsymbol{\tau}_l^T \tilde{\boldsymbol{\gamma}}_{\boldsymbol{x}_l} - \boldsymbol{\eta}_l^T \boldsymbol{z}_l$, respectively.

As can be seen, the master problem (M) might be non-convex and is in general complex to solve, as it is a mixed-integer problem. However, note that it can easily be transformed into a purely integer problem when the utility functions $U_i(r_i)$ are non-decreasing, which is the case for the most commonly used functions, e.g., weighted sum-rate or proportional fair rates, and $\boldsymbol{h}(\boldsymbol{r})$ enforces minimum rate constraints, which is an often made assumption in literature. In this case, the constraints (2c) and (2d) can be assumed tight at optimality, because lower rates do not produce larger utility. Thus, equations (2a)-(2d) may be replaced with two lines as

$$\max_{\boldsymbol{x},\boldsymbol{p},\boldsymbol{y}} \sum_{i\in\mathcal{L}} U_i\left(\sum_{k\in\mathcal{R}} \boldsymbol{d}_i^T \boldsymbol{x}_i^{(k)}\right) \text{ s.t. } \boldsymbol{h}\left(\sum_{k\in\mathcal{R}} \boldsymbol{d}_i^T \boldsymbol{x}_i^{(k)}\right) \leq \boldsymbol{0}. \quad (32)$$

**Algorithm 1** Semi-Decentralized Scheduling

```
Choose utilities U_i(r_i) and constraints h(r), g(x)
Choose p for ℓ^p norm, T > 0, ε > 0, set l := 0.
Initialize bounds as: UB := ∞, LB := −∞
while UB − LB ≥ ε do
    l := l + 1
    Solve (M), yielding x_l, r.
    Set UB := min{UB, Σ_{i∈L} U_i(r_i)}
    Communicate x_l to all links
    Initialize p[1] := p̄
    for t = 1,...,T do
        Transmit with p[t], using MCS x_l
        Rx's feed back SINRs Γ_i^(k)(p[t]) to Tx's
        Set p_i^(k)[t+1] := min{p_i^(k)[t] γ^(k)_{x_l,i} / Γ_i^(k)(p[t]), p̄_i^(k)}
    end for
    Tx's report SINRs Γ_i^(k)(p[T]) to BS
    Add constraint ξ_l(x) ≤ 0 to (M) according to (30)
    Set x̂_{q_i}^(k) := 𝟙{q_i = arg max{r_{q_i} : Γ_i^(k)(p[T]) ≥ γ_{q_i}}}
    Set r̂_i = Σ_{k∈R} r_i^T x̂_i^(k)
    Set LB := max{LB, Σ_{i∈L} U_i(r̂_i)}
end while
Output: x̂, p[T].
```

i.e., the variables $\boldsymbol{r}$ are not part of the optimization anymore. Further, the logarithm in (31) can be approximated by defining a vector $\tilde{\overline{\boldsymbol{\gamma}}} = \log \overline{\boldsymbol{\gamma}}$ and a parameter $\theta \ggg 0$, yielding

$$\log(\overline{\boldsymbol{\gamma}}_i^T \boldsymbol{x}_i^{(k)}) \approx \tilde{\overline{\boldsymbol{\gamma}}}_i^T \boldsymbol{x}_i^{(k)} - \theta\left(1 - \boldsymbol{1}^T \boldsymbol{x}_i^{(k)}\right). \quad (33)$$

As long as $\boldsymbol{1}^T \boldsymbol{x}_i^{(k)} = 1$, the approximation is exact, yielding the SINR target of chosen MCS in logarithmic domain. Only if no MCS is chosen, the approximation is not exact, as the actual value would by minus infinity, effectively deactivating the respective constraint in (31). By choosing $\theta$ large enough, this behavior can be reproduced, leading to an equivalent formulation.

## IV. ALGORITHM & PERFORMANCE STATEMENTS

From the applied GBD, we can derive a semi-decentralized scheduling mechanism as shown in Algorithm 1 and, more comprehensively, in the flow-chart of Figure 2. The intuition is as follows: At first, the scheduling problem is solved at the BS, neglecting completely the SINR constraints (2h)-(2j). The resulting schedule and MCS assignment is communicated to the transmitters, which derive the associated SINR targets. Then, the power-constrained FM-PCA is run for $T$ iterations and the last measured SINR values are reported back to the BS. The BS adds a constraint of the form $\xi_l(\boldsymbol{x}) \leq 0$ to the master problem and by this incorporates an estimate for which MCS combinations can be achieved with the current channel state into future scheduling instances. For example, if the SINR constraints of an MCS assignment could not be satisfied, this particular assignment and some more infeasible assignments are eliminated from all future schedules. With this additional constraint, a new schedule

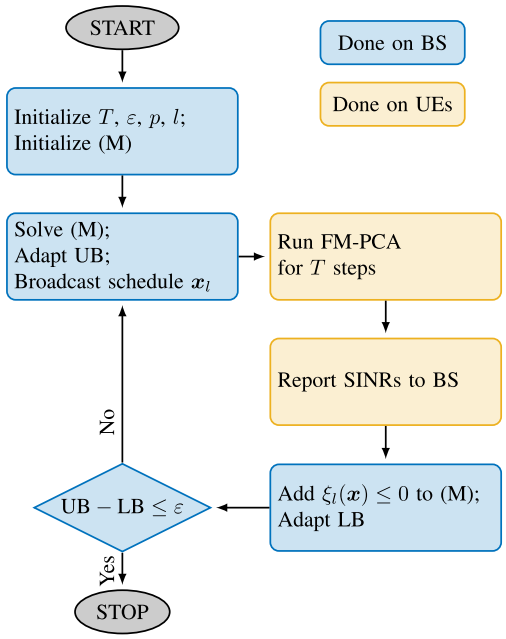


**FIGURE 2.** Flowchart of Algorithm 1.

is calculated and the whole procedure is repeated. In the course of repetitions, the space of feasible MCS assignments is explored and bounded until it is known well enough to find a close-to-optimal schedule. To evaluate how close the quality is to the optimum solution, an upper bound UB and lower bound LB of the optimal utility are tracked during algorithm execution. The UB thereby considers the smallest so far targeted utility as outcome of the master problem (M), i.e., the smallest observed upper bound to the optimum, while the LB considers the largest actually achieved utility as result of the PCA, which is the largest observed lower bound. When UB and LB are within a tolerable range $\varepsilon$, the algorithm terminates.

### A. PERFORMANCE STATEMENTS

We will now present performance statements of proposed Algorithm 1. For this, we define the sets $\mathcal{F}_X = \{\boldsymbol{x} \mid \exists \boldsymbol{\gamma}, \boldsymbol{p} : \text{(2e)-(2j)}\}$ and $\mathcal{F}_l = \{\boldsymbol{x} \mid \text{(2e)-(2g)}, \ \xi_n(\boldsymbol{x}) \leq 0 \ \forall n < l\}$. While $\mathcal{F}_X$ denotes the actual set of feasible $\boldsymbol{x}$, i.e., MCS assignments that satisfy all scheduling constraints and can be satisfied for a valid power vector, the set $\mathcal{F}_l$ denotes the valid MCS assignments at the $l$'th instance of (M), respectively. Note that by design, it holds that $\mathcal{F}_l \supseteq \mathcal{F}_X \ \forall l$ [32].

*Proposition 6:* For increasing $T$, the result of the for loop in lines 10-14 converges towards an optimal solution of (F) with linear rate.

*Proof:* It is a well established result of power control theory [8], [30], [34], [36] that the loop in lines 10-14 converges to a unique fixed point with linear rate. As we have shown in Proposition 4, the fixed point is an optimal solution to (F). ∎

Note that more specific convergence bounds can be derived by using results from Perron-Frobenius Theory [30], particularly stating the accuracy of obtained multipliers. However, these are out of the scope of this work and depend heavily on the actual channel coefficients, more precisely on the spectral radius of the relative gain matrix [30]. Sufficiently good values for $T$ must therefore be derived by experience in practice.

*Proposition 7:* For any $T < \infty$, proposed Algorithm 1 terminates within a finite number of steps when $\varepsilon > 0$, and even when $\varepsilon = 0$.

*Proof:* Consider the constraints $\xi_l(\boldsymbol{x})$ given in (30), which are added after each instance of (F). By using the definitions, it must hold that $\log(\overline{\boldsymbol{\gamma}}_i^T \boldsymbol{x}_{l,i}^{(k)}) = \tilde{\gamma}_{\boldsymbol{x}_l,i}^{(k)} \ \forall i, k$ and hence $\xi_l(\boldsymbol{x}_l) \geq 0$, with equality if, and only if, $z_i^{(k)} = 0 \ \forall i, k$. As result, it holds that $\mathcal{F}_{l+1} \subseteq (\mathcal{F}_l \setminus \boldsymbol{x}_l)$, i.e., $\boldsymbol{x}_l$ is removed from the domain of (M) for any future instance if it was infeasible. Now observe that the set $\mathcal{F}_1$, defined simply by (2e)-(2g), is finite and that LB $=$ UB holds whenever $\boldsymbol{x}_l$ is found to be feasible, triggering the termination of the algorithm. Assume that the algorithm would never terminate. Then at each instance, at least one vector $\boldsymbol{x}_l$ is removed from the finite domain of (M), thus at some point, it would have to be empty, rendering the (M) infeasible. As optimization over an infeasible space yields UB $:= -\infty$, the termination criterion would be met, contradicting the assumption that the algorithm does not terminate. ∎

Propositions 6 and 7 together create the picture that increasing $T$, the accuracy of solving (F) is increased, which also increases the accuracy of obtained bounds $\xi_l(\boldsymbol{x})$. However, even for low $T$, the algorithm will always terminate and produce an output result. Although this tells nothing about the actual complexity, nor on the quality of the produced output, it guarantees a well-defined functionality in any case, as the algorithm will never be caught in a deadlock.

*Proposition 8:* Assume an algorithm for solving (M) that, for each instance $l$, is guaranteed to produce a solution $(\boldsymbol{x}_l, \boldsymbol{r}_l)$ with utility $U(\boldsymbol{r}_l) \geq \alpha U(\boldsymbol{r}_l^*) - \beta$, where $(\boldsymbol{x}_l^*, \boldsymbol{r}_l^*)$ is the optimal solution to the $l$'th instance of (M), $\alpha \in [0, 1]$ and $\beta \geq 0$. Then, using this algorithm for solution of (M) and for $T$ large enough, upon termination Algorithm 1 will produce a solution $(\boldsymbol{x}', \boldsymbol{r}')$ such that $U(\boldsymbol{r}') \geq \alpha U(\boldsymbol{r}^*) - \beta - \varepsilon$.

*Proof:* If $T$ is large enough, the result of the PCA converges arbitrarily close the optimal solution of (F) or (P) due to convergence with linear rate. Assume $T$ it to be so large that the solution inaccuracy is negligible. Let $\text{UB}[l] = \min\{\text{UB}[l-1], U(\boldsymbol{r}_l')\}$ with $\text{UB}[0] := \infty$ be the upper bound obtained from the $l$'th instance of (M) with the approximation. It holds $\forall l$ that

$$\begin{aligned} \text{UB}[l] &= \inf\{U(\boldsymbol{r}_1'), \ldots, U(\boldsymbol{r}_l')\} \\ &\geq \inf\{\alpha U(\boldsymbol{r}_1^*) - \beta, \ldots, \alpha U(\boldsymbol{r}_l^*) - \beta\} \\ &\geq \alpha U(\boldsymbol{r}^*) - \beta. \end{aligned} \tag{34}$$

The last inequality holds because each instance of (M) is a relaxation to the original problem, as $\mathcal{F}_l \supseteq \mathcal{F}_X \ \forall l$, and hence $U(\boldsymbol{r}_l^*) \geq U(\boldsymbol{r}^*) \ \forall l$. As the algorithm terminates when $U(\boldsymbol{r}') = \text{LB}[l] \geq \text{UB}[l] - \varepsilon$, the result holds. ∎

In particular, by choosing $\alpha = 1$, $\beta = 0$ and $\varepsilon = 0$, Proposition 8 states that when the master problem is solved optimally, Algorithm 1 converges to the optimal solution of the targeted problem. Concluding this section, Algorithm 1 has the properties that (i) it always terminates in a finite number of steps, (ii) approximation statements that can be made for the master problem transfer to the overall solution and (iii) the larger $T$, the more precise the solution of the feasibility problem becomes.

### B. OVERHEAD & COMPLEXITY

We stated already that the problem we investigate is generally NP-complete, due to the coupling of the binary decision variable with SINR-constraint. Because we show that our approach allows optimal solution, we cannot expect it to run fast for all instances and remain optimal. At this level of generality, the only analytic complexity statement we can make is that the overall complexity is $\Omega(K \cdot \Omega((M)))$, where $\Omega((M))$ is the complexity of (M) and $K$ is the required number of outer iterations. While we might give values for $\Omega((M))$ in specific cases, $K$ is in general unknown. We will therefore assess it in the simulative analysis in Section V.

As for information exchange, Algorithm 1 contains (i) the broadcast of a schedule of $|\mathcal{L}||\mathcal{R}|$ numeric values in line 8 after each master problem solution, (ii) $|\mathcal{L}||\mathcal{R}|$ SINR reports from receiver to transmitter per PCA step in line 12 and (iii) $|\mathcal{L}||\mathcal{R}|$ final SINR reports in line 15. So if the algorithm requires $K$ outer iterations and has $T$ PCA steps per iteration, the overall reports require transportation of $K(T+2)|\mathcal{L}||\mathcal{R}|$ numeric values over signaling channels. As the algorithm runs for $KT$ slots, on average $(1 + 2/T)|\mathcal{L}||\mathcal{R}|$ values are transported per slot. Note that the reporting overhead grows linearly with the number of links. In comparison, the average overhead of full channel measurement reporting that is done every $K$ slots in the order of $\Omega(|\mathcal{L}|^2|\mathcal{R}|/K)$ per slot [4], as all channel values need to be communicated to the base station.

### C. SOLVING A PARTICULAR MASTER PROBLEM

Due to our general formulation, clearly we cannot expect to give a solution that applies to all cases of (M). We therefore investigate solution of a particular problem, which is that of Weighted Sum-Rate (WSR) maximization with minimum connectivity demands for cellular links. We stress that our previous performance assessment remains valid for a large range of problems, such that we can use Algorithm 1 in a variety of set-ups by just changing the way the master problem is solved in line 6, respectively.

Mathematically, WSR maximization corresponds to (M) with $U_i(r_i) = w_i r_i \; \forall i$, where $w_i \geq 0$ is a weighting factor, and an empty $\boldsymbol{h}(\boldsymbol{r})$. Using (32) and (33), defining as $\mathcal{C} \subseteq \mathcal{L}$ the set of cellular uplinks, as $\mathcal{D} \subseteq \mathcal{L} \setminus \mathcal{C}$ that of D2D links and setting $\mathcal{R}_i = \mathcal{R} \; \forall i$, we can formulate the problem as:

$$\text{(WSR-M)} \quad \max_{\boldsymbol{x},\boldsymbol{r}} \sum_{i\in\mathcal{L}} \sum_{i\in\mathcal{L}} w_i \sum_{k\in\mathcal{R}} \boldsymbol{d}_i^T \boldsymbol{x}_i^{(k)} \quad \text{s.t. (2e)-(2g)},$$

$$1 - \sum_{k\in\mathcal{R}} \sum_{q\in\mathcal{X}_i} x_{qi}^{(k)} \leq 0 \quad \forall i \in \mathcal{C}, \tag{35a}$$

$$\sum_{i\in\mathcal{C}} \sum_{q\in\mathcal{X}_i} x_{qi}^{(k)} - 1 \leq 0 \quad \forall k \in \mathcal{R}, \tag{35b}$$

$$\sum_{i\in\mathcal{L}} \sum_{k\in\mathcal{R}} \tau_{n,i}^{(k)} (\tilde{\overline{\boldsymbol{\gamma}}}_i + \theta \mathbf{1})^T \boldsymbol{x}_i^{(k)} - W_n - \theta \sum_{i\in\mathcal{L}} \sum_{k\in\mathcal{R}} \tau_{n,i}^{(k)} \leq 0 \quad \forall n \leq l. \tag{35c}$$

Note that the constraints (35a)-(35c) are instances of the scheduling constraint vector $\boldsymbol{g}(\boldsymbol{x})$. Constraint (35a) ensures that all cellular links remain connected, i.e., may choose at least one MCS on a PRB, while (35b) demands that not more than one uplink uses a PRB and (35c) is a reformulation of the master constraints (31) that were adapted using (32) and (33). For ease of notation, we use $g_n(\boldsymbol{x}) \leq 0$ to refer to the $n$'th instance of (35c) in the following.

Problem (WSR-M) takes the form of a multi-dimensional Knapsack problem, which is hard to solve exactly. However, we can approximate it in the following fashion: In addition to the constraints given in (WSR-M), we add a scheduling mask of the form $\boldsymbol{x} \leq \hat{\boldsymbol{x}}_l$ with $\hat{x}_{l,qi}^{(k)} \in \{0,1\} \; \forall q,i,k$ to the $l$'th master problem instance, that forbids certain links the use of specific MCS on specified PRBs. We begin with $\hat{\boldsymbol{x}}_0$ such that $\hat{x}_{0,q_i i}^{(k)} = \mathbb{1}\{\tau_{n,i}^{(k)} \overline{\gamma}_{q_i} \leq W_n \; \forall n \leq l\}$, which allows each link to use any MCS setting of maximum rate that alone would not violate a $g_n(\boldsymbol{x})$. Then, for each master constraint $g_n(\boldsymbol{x})$, $n \leq l$, in (35c), we construct the vector $\overline{\boldsymbol{x}}_n = [\overline{\boldsymbol{x}}_{n,1}^T, \ldots, \overline{\boldsymbol{x}}_{n,L}^T]^T$ with $\overline{x}_{n,q_i i}^{(k)} = \mathbb{1}\{q_i = \sup\{q_i \in \mathcal{X}_i \mid \hat{x}_{n-1,q_i i}^{(k)} = 1\}\}$, that indicates the maximum allowed MCS, and search for the resource-link combination of maximum weight $(i^*, k^*) = \arg\max_{i,k}\{\tau_{n,i}^{(k)}\}$. From this we construct $\hat{\boldsymbol{x}}_n = [\hat{\boldsymbol{x}}_{n,1}^T, \ldots, \hat{\boldsymbol{x}}_{n,L}^T]^T$ by assigning $\hat{\boldsymbol{x}}_{n,j} = \hat{\boldsymbol{x}}_{n-1,j} \; \forall j \neq i^*$ and $\hat{\boldsymbol{x}}_{i^*} := \boldsymbol{f}_n(\overline{\gamma}^*)$, where $\boldsymbol{f}_n(\overline{\gamma}^*)$ is a vector valued function with the elements $\hat{f}_{q_i}(\overline{\gamma}^*) := \mathbb{1}\{\overline{\gamma}_{q_{i^*}} \leq \overline{\gamma}^*\} \; \forall q_{i^*}$ and $\overline{\gamma}^*$ is chosen to satisfy $\overline{\gamma}^* = \sup\{\overline{\gamma}_{q_i} : g_n(\overline{\boldsymbol{x}}_{n+1}(\overline{\gamma}_{q_i})) \leq 0\}$. In words, for the resource-link combination with maximum weight, we search for the maximum MCS that would not violate $g_n(\boldsymbol{x})$ if all other links choose their maximum allowed MCS. Note that we can always find a $\overline{\gamma}^*$ such that $g_n(\hat{\boldsymbol{x}}_l) \leq 0$: If the right hand side set of its assignment is empty, $\overline{\gamma}^* = -\infty$ and $\hat{x}_{l,q_{i^*}i^*}^{(k^*)} = 0 \; \forall q_{i^*} \in \mathcal{X}_{i^*}$. In this case, because of the effect of $\theta$ discussed around (33), $g_n(\hat{\boldsymbol{x}}_l) \leq 0$ holds true.

Because the constraint $\boldsymbol{x} \leq \hat{\boldsymbol{x}}_l$ allows only allocations that satisfy $g_n(\hat{\boldsymbol{x}}_l) \leq 0$, the master constraints (35c) become obsolete. The remaining problem can be split into two independent problems, one for the cellular links that includes constraints (35a)-(35b) and one for the D2D links. The cellular link problem can be transformed into weighted bipartite matching problem that can be solved in $\Omega(|\mathcal{C}|^3|\mathcal{R}|^3)$ operations using the Hungarian method of Kuhn [38] and Munkres [39], while the D2D link problem can be solved optimally in $\Omega(|\mathcal{D}||\mathcal{R}|)$ operations by using a greedy assignment on each PRB. As we will show now, the optimal solution of the adapted problem is an approximation of the master problem:

*Proposition 9:* Denote by (WSR-M-A) the adapted version of (WSR-M) with $l$ constraints, where (35c) is replaced by $\boldsymbol{x} \leq \hat{\boldsymbol{x}}_l$ with $\hat{\boldsymbol{x}}_l$ adapted as discussed above. Then the optimal solution (WSR-M-A) approximates that of (WSR-M) with $\alpha = 1$ and $\beta = l \cdot \max_{i,q}\{w_i d_{qi}\}$.

*Proof:* For each of the $l$ constraints $g_n(\boldsymbol{x}) \leq 0$, $n \leq l$, in the worst case one link is unnecessarily completely deactivated, which might reduce the WSR at most by $\max_{i,q}\{w_i d_{qi}\}$ compared to the actual optimum. ■

## V. SIMULATION RESULTS

To showcase the validity of the proposed structure, we present simulation results for the discussed weighted sum-rate utility in a scenario where D2D is allowed to use uplink bands. For the sake of transparency, the entire tool-chain used for simulation and evaluation, as well as the raw result data are made available at [40].

A single cell is considered with six frequency channels of 180 kHz width that are placed with center frequencies of 2 GHz and larger and a slot-length of 1 ms. A predetermined number of D2D links are distributed on a spatial area of 500m × 500m, with the BS at the center and a maximum D2D distance of 25 m. With each D2D link, an uplink UE is added to the network, however, the total number of uplink UEs is upper bounded to the number of frequencies (i.e., six) to guarantee existence of a dedicated channel for each. Channel attenuation is generated according to scenario C2 (Urban Macro) of the Winner-II model [41], which takes into account the distance based path loss, line-of-sight probability and shadowing, based on the devices' antenna heights. Different MCS are used, corresponding to Long Term Evolution (LTE) MCS, which range from Quadrature Phase Shift Keying (QPSK) to 64 - Quadrature Amplitude Modulation (64-QAM). Each MCS is associated with a data rate and minimum SINR target according to [42, Appendix A2]. Whenever an MCS is chosen, the associated SINR target was activated to guarantee a defined performance. In general, it was assumed that each UE uses at most one channel.

In this set-up, a sum-rate maximization problem was optimized, using the proposed GBD-based method. Three different reuse-policies were targeted: i) One-Fold Reuse (OFR): Here, each channel is to be used at most by one D2D link and under the constraint that all uplink UEs can achieve at least the SINR of the minimum-rate MCS. ii) Multi-Fold Reuse (MFR): Here, each channel may be used by any D2D link, again under the constraint that all uplink UEs can achieve at least the SINR of the minimum-rate MCS. iii) Arbitrary Reuse (AR): Similar to MFR, AR allows the channels to be used by any D2D link but drops the uplink SINR guarantees.

Before starting the comparison, we performed an impact analysis of the used $\ell^p$ norm and number of PCA iterations $T$, which we unfortunately cannot show due to space restrictions. The result is that the achieved sum-rate is in general independent of $p$. However, we use $p = 2$ in the following due to fastest convergence. Further, to our surprise, the achieved sum-rate does not improve significantly after $T \geq 2$ and fastest convergence can be achieved for $T = 2$. This is an important practical insight, because theoretically, we can only prove that $T$ needs to be ''sufficiently large''. However this sufficiency is given already after very few PCA iterations.

### A. GENERAL PERFORMANCE

Using the approximate solution to (M) as presented in Section IV-C, we compare OFR, MFR and AR for the a SC-FDM use-case, in which each link is restricted to use a single channel. The algorithm performance in terms of sum-rate, convergence delay and achieved reuse factor is depicted in Figure 3, where all data points represent averages over network 1000 realizations. In Figure 3a we show the achieved sum-rate, together with an upper bound that we achieved by directly relaxing the integer constraint for each master problem. Note that this upper bound is not tight but overestimates the achievable rate. Figure 3b shows the required delay to termination, including the time for PCA but excluding optimization, and 3c the achieved reuse-factor, which is the total number of allocated links divided by the number of channels. Figure 3c further shows the maximum reuse factor on a single channel, achieved over all Monte-Carlo runs by either OFR, MFR or AR. Surprisingly, MFR and AR show almost equal performance. This is counter-intuitive, as technically AR is a relaxation to MFR that allow reducing the performance of uplinks to enable larger sum-rate by increased frequency reuse. However, as both are close to the upper bound of AR, we conclude that not much performance can be gained by shutting down the cellular links.

It can be seen in the figures that for one-fold reuse, the performance converges to a fixed value early. An average reuse factor of two is achieved for 15 links and more, however, it also needs only four milliseconds (two master problem instances) for convergence over the full range of links. For MFR and AR, the sum-rate increases linearly over the considered link range, which indicates that the number of links could in principle be increased further, as the network is not saturated yet. In fact, our analysis shows that saturation effects slowly at begin around 200 nodes. Algorithm delay increases slightly more than linearly and achieves the mark of 100 ms, corresponding to a typical coherence time for low-movement scenarios, at around 100 links. Finally, the increase in reuse factors can be seen in Figure 3c. While OFR allows reuse factors of up to two, with MFR and AR the average reuse increases to 16 for one hundred links. Even further, the maximum reuse factor reached throughout all simulation runs grows to 30 for 100 links, which is indeed an order of magnitude more than the typically targeted one-fold reuse. Note that the OFR case poses an upper bound to a series of works [9]–[11], [14], [18], [20], [25], which therefore must achieve lower performance compared to ours.

Figure 4 shows the mean computational delay for solution of the master problem (M), again averaged over 1000 instances. Note that the optimization was performed on an Intel i7 core with 3.6 GHz clock frequency and executed in Matlab using custom-built code that was not optimized for speed. Surprisingly, it can be seen that OFR has the longest optimization delay and is in the order of several ms after about 25 links, while the optimization delay for MFR and AR remain below 10 ms for the whole domain. While this is

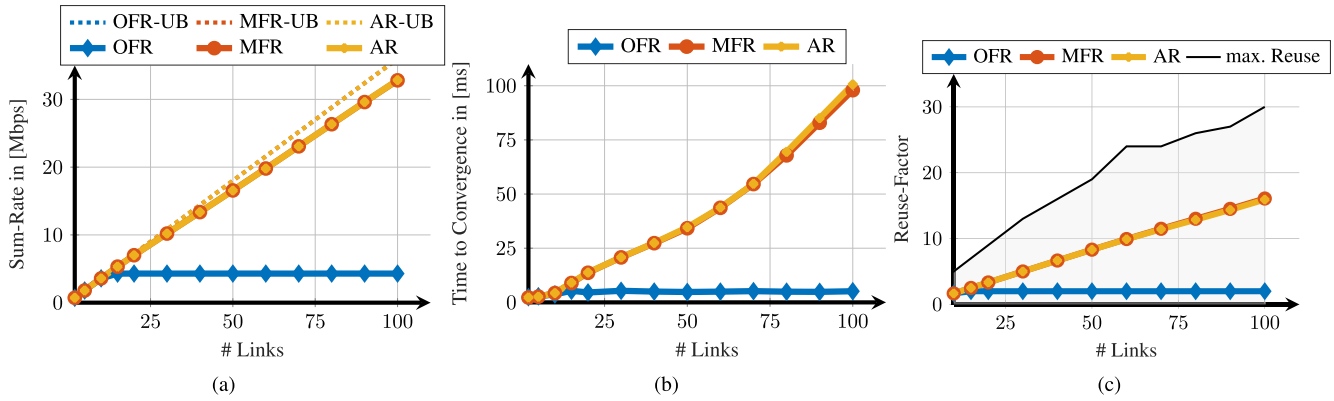


**FIGURE 3.** Simulation results for a sum-rate maximization problem in an SC-FDM scenario with the different interference constraints of One-Fold Reuse (OFR), Multi-Fold Reuse (MFR) and Arbitrary Reuse (AR). Note that the OFR case poses an upper bound to the performance of works [9]–[11], [14], [18], [20], [25].

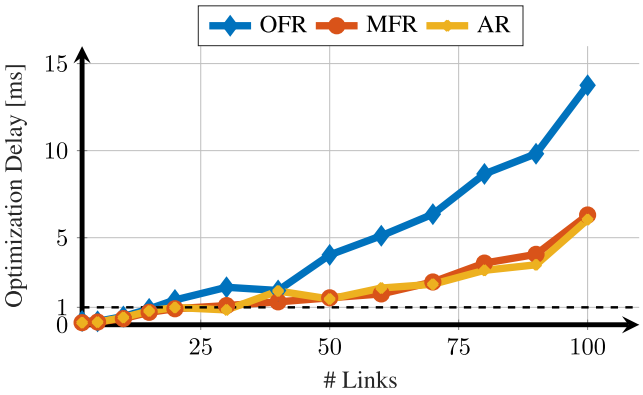


**FIGURE 4.** Mean computation delay for the instances of (M) using an unoptimized Matlab code. OFR shows worst performance, because it requires that all D2D pairs are optimized with the Hungarian method, while MFR and AR allow greedy allocation of D2D links as explained in Section IV-C.

counter-intuitive at first, it results from the fact that for OFR the Hungarian method is used to solve the D2D allocation, which creates a significant burden as the number of links increases. For MFR and AR, as explained in Section IV-C, a greedy allocation is sufficient due to the introduced approximation, such that the main delay originates from identifying the maximum-weight link on each channel and adding constraints according to Section IV-C. Note that the Matlab software, while handy, is not known for its efficiency and also we did not invest effort to optimize the code for speed. It can therefore be expected that the optimization delay may be reduced by at least one order of magnitude when using an optimized C++ implementation and even further when the optimization is implemented on a hardware platform. We therefore conclude that with our approximative solution for the weighted sum-rate maximization, it is realistic to consider optimization delay as negligible.

### B. COMPARISON TO EXISTING METHODS

We now compare our proposed method to the a centralized, heuristic scheme of Zhao and Wang [17] and the decentralized pricing scheme of Yin *et al.* [21], which we consider as closest related works. Compared to our previous investigation, both works investigate an Orthogonal Frequency Division Multiplex (OFDM) D2D scenario, in which D2D links may use an arbitrary number of channels and adapt their powers dynamically. While Zhao and Wang [17] solve the problem by heuristically forbidding reuse among links, Yin *et al.* [21] cast it to a power control problem that they solve with game theory. Note that both works optimize the Shannon bound and hence assume an implicit MCS selection that achieves capacity, while we assume imperfect MCS and explicitly set the MCS in our problem. Therefore our schemes are not directly comparable. To overcome this, we use the final power allocations to obtain the link SINRs after employing the solutions of [17], [21] and assign each link the maximum MCS that it can use with this SINR in retrospective.

Figure 5 shows the comparison in terms of achieved sum-rate, required algorithm delay and control traffic. Because the work of Zhao and Wang [17] assumes full parameter knowledge while the others do not, we incorporated the delay and reporting traffic of channel sounding into the calculation. It can be seen from Figure 5a that all curves have a concave appearance, which can be explained by the fact that, as the network becomes more congested, all algorithms tend to choose lower-rate MCS. Our proposed algorithm outperforms the other works significantly in terms of achieved rate, while that of Yin *et al.* [21] also outperforms that of Zhao and Wang [17]. In terms of delay, shown in Figure 5b, the decentralized method of Yin *et al.* [21] is extremely fast, converging after only eight ms for the full range of links. However, it must also be noted that this performance is vulnerable to misconfiguration - when using the parameters given in the original work, the algorithm had severe convergence issues that would push the convergence time out of bounds in our plot. The scheme of Zhao and Wang [17] requires a linear time to sound all channels – each transmitter must transmit once on all channels – and our proposed scheme shows linear delay increase for large number of links. Finally, we compare the produced control traffic in Figure 5c. For this, we calculated the required number of numeric values for reporting and broadcasting and converted them into a data

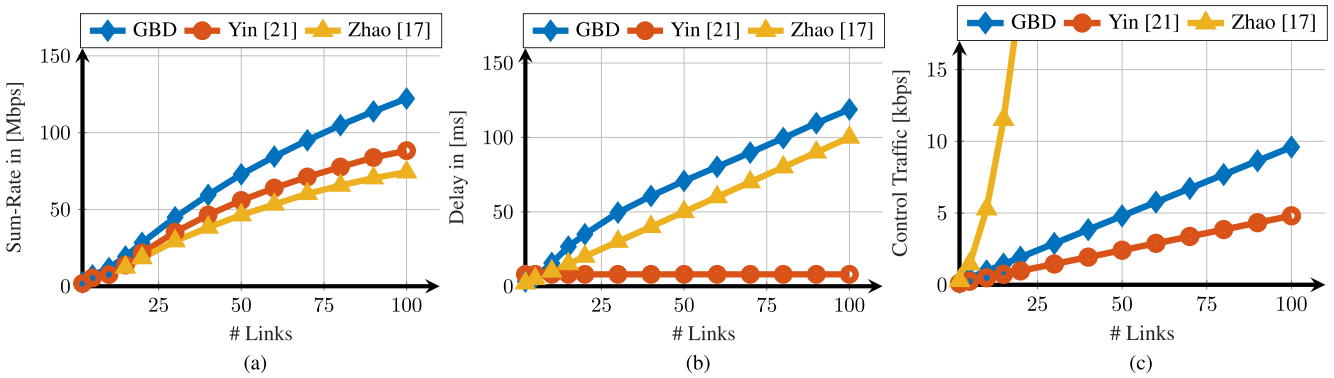


**FIGURE 5.** Simulation Results for a sum-rate maximization problem with OFDM D2D-Links. Fig. 5a shows the average achieved sum-rate per number of links, 5b the algorithm delays and 5c the induced control traffic.

rate by assuming that each value is represented by a single byte and then dividing the resulting total amount of bytes by the algorithm delay. It can be seen that central channel reporting used by Zhao and Wang [17] is inefficient, as the traffic grows quadratically with the number of links. Both our proposed scheme an that of Yin *et al.* [21] show linear increase, however, the algorithm of Yin *et al.* [21] has a better scaling factor.

In Figure 6, we show the time-delay added to each iteration by central calculations at the BS for the different schemes. As before, all optimizations were performed on an Intel i7 core with 3.6 GHz clock frequency and executed in Matlab using custom-built code. The main source of overhead for Yin *et al.* [21] comes from the calculation of an appropriate pricing vector at the base station. Note that some pre-calculations need to be done once at the very beginning of the optimization, such as calculation of the schedule for cellular devices. We reflected this by distributing the delay of these evenly over all iterations, which explains the delay decrease for few links. For our proposed GBD-based method, the overhead comes from the creation of constraints $\xi_l(\boldsymbol{x}) \leq 0$ from SINR reports, the application of the approximation procedure introduced in Section IV-C and the resulting greedy MCS allocation. In contrast, for Zhao *et al.* [17] the full scheduling algorithm is run in a single-shot procedure, which includes calculation of optimal transmission powers for each 3-tuple of devices and the choice of the optimal allocation afterwards. It can be seen from Figure 6 that the scheme of Yin *et al.* [21] has lowest computation overhead and is in sub-ms range, while our algorithm takes up to 14 ms for the solution of each (M) instance. The solution of Zhao *et al.* [17] adds a single-shot delay of up to 1s for calculating a schedule. Note that again, we did not optimize the Matlab code for speed, such that an implementation in C++ or hardware would reduce the delays by at least one order of magnitude. For such an optimized implementation, our proposed scheme maintains good speed over most of the link range.

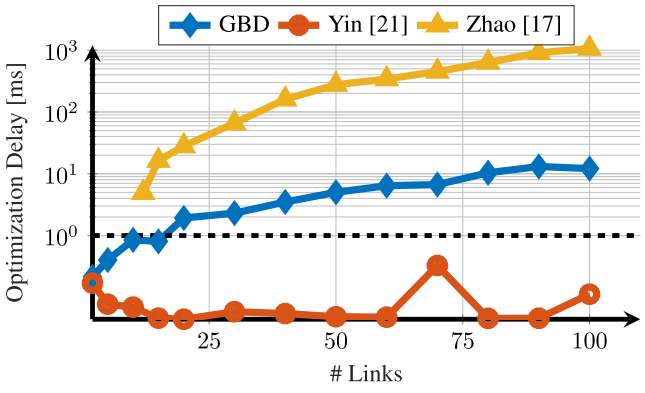


**FIGURE 6.** Mean computation delay per iteration for schedule creation in the different algorithms using Matlab.

Concluding, the centralized scheme of Zhao and Wang [17] achieves worst performance at moderate delays and large reporting overhead, while the decentralized method of Yin *et al.* [21] is a slim and powerful scheme. However, it is still beaten in performance by our proposed algorithm, which also has moderate delay and low reporting overhead. The reason why we still out-perform Yin *et al.* [21] lies in the fact that they approximate the rate by using the Shannon capacity formula. This renders the variable space continuous and allows them to use a performant iterative waterfilling method. However, it is based on a coarse approximation of the real rate. On the other hand, we use a more realistic rate model with explicit MCS selection. This allows us to achieve full performance but at the cost that the problem becomes combinatorial, in which case game theoretic approaches typically have converge issues. Still, we are able to compare with the decentralized scheme in all aspects except for the delay, which we consider a strong performance.

### C. COMPARISON FOR VARYING CHANNELS

Finally, we compare to the works of Zhao and Wang [17] and Yin *et al.* [21] in a varying channel scenario with 50 links. For this, we kept the positions of nodes fixed and pre-defined a channel coherence time. Within a coherence time we kept the channels static and after a coherence time passed, they were re-generated with independent, identically distributed values.

As our scheme relies on the consecutive approximation of the feasible space, it is clear that when the channel changes, this approximation must become inaccurate. We solved this

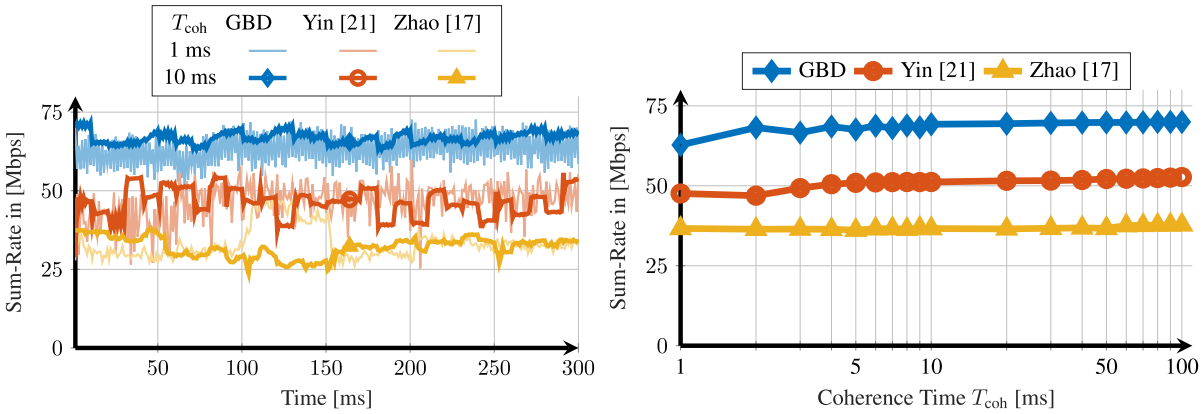


**FIGURE 7.** Algorithm performance under varying channels and for 50 links. Fig. 7a shows a single network instance with 1 and 10 ms coherence time, while Fig. 7b shows the performance dependency on the channel coherence time.

by defining a "maximum memory time" for the constraints and dropping constraints that were older than this threshold time. We used a maximum memory time of 25 ms throughout our simulations. For the scheme of Zhao and Wang [17], which relies on full parameter knowledge, we assumed a continuous channel sounding, in which the channel coefficients of one link towards all other links are refreshed in a round-robin fashion.

The results of our comparison are shown in Figure 7. The performance on a single sample with coherence times $T_{\text{coh}}$ of 1 ms and 10 ms is shown in Figure 7a. It can be seen from the curve of 10 ms that the algorithm of Yin *et al.* [21] adapts extremely fast after new channels are generated. Compared to this, our scheme also shows a following behavior while that of Zhao and Wang [17] has problems to adapt. Interestingly, the performance of all algorithms remain comparable to the static case, with our scheme out-performing the others. This is particularly true for $T_{\text{coh}} = 1$ ms, which corresponds to an i.i.d channel variation. While all algorithms show performance variations here, the general order of performance magnitude remains the same. In Figure 7b we show the performance dependency on channel coherence times by comparing the average rate achieved over 300 ms and 200 different network realizations. Surprisingly, there is little to no dependency for any of the algorithms, even down to the very low coherence times of 1s.

### D. WAYS TOWARDS MULTICELL SYSTEMS

In this work we made a single-cell assumption in order to have a well-defined system. However, in reality D2D interference problems can span multiple cells, rendering the problem even more challenging. From a purely mathematical perspective, the formulation of a full-fledged multicell scheduling problem is a variant of (2) in which the set of UEs is simply extended to cover multiple cells. Therefore, it would also be possible to extend our proposed procedure to multicell systems. However, in practice this would require a multicell scheduler, i.e., a central entity that makes joint scheduling decisions for multiple cells. This is rather unrealistic considering the number of UEs such a scheduler would have to deal with and the time scale at which scheduling is done. Alternatively, it could be possible to split Algorithm 1 into independent subroutines that would run on different entities. This could be done, e.g., by using an on-line spectrum partitioning among cells (this would adapt $\boldsymbol{g}(\boldsymbol{x})$ and $\mathcal{R}_i$) or by identifying UE groups that have negligible mutual cross-group interference coupling and optimizing solely among each group. Both methods would allow (2) to be divided into independent sub-problems that can be solved on BS level. Unfortunately, the investigation of methods for this kind of adaptation is out of the scope of this article, such that we leave this topic open for future work.

## VI. CONCLUSION

We conclude by summarizing the main insights gained in this article. An interference aware scheduling problem for a D2D-enabled cellular network was investigated, with a level of generality that makes it applicable to overlay, underlay, uplink and downlink D2D for various utility functions and scheduling constraints. By applying a Generalized Benders Decomposition, the problem was split into a power control problem and a scheduling problem. The power control problem was shown to be solved by a Foschini-Miljanic type algorithm, which is decentralized and based on SINR measurements instead of channel measurements. The master problem, on the other hand, is a traditional scheduling problem without interference constraints. We established an optimization flow and reporting structure that can be used to solve interference aware resource allocation for D2D communication in various setups. Convergence properties of the overall procedure were established by stating that independent of the exact constraints and optimization goal, the algorithm terminates in a finite number of steps and that approximations on the master problem transfer to the overall solution. Simulations verified the theoretic statements and showcased the amount of reuse that can be achieved by releasing the constraint of one-fold reuse. In particular, in the given simulation set-up up to 31-fold frequency reuse was achieved within a single cell, which is by an order of

magnitude larger than the often assumed one-fold reuse. Further, we proposed an explicit approximative solution for the weighted sum-rate maximization problem and compared our algorithm with existing state of the art. It could be seen that our algorithm outperforms existing work by around 35% while still achieving reasonable convergence and signaling overhead. Although designed for static channels, our algorithm also outperforms existing works in variable channel setup. In summary, the proposed algorithm is semi-decentralized, allows flexible adaptation to various network configurations and enables well-defined performance.

## REFERENCES


[1] A. Asadi, Q. Wang, and V. Mancuso, "A survey on device-to-device communication in cellular networks," *IEEE Commun. Surveys Tuts.*, vol. 16, no. 4, pp. 1801–1819, 4th Quart., 2014.

[2] P. Mach, Z. Becvar, and T. Vanek, "In-band device-to-device communication in OFDMA cellular networks: A survey and challenges," *IEEE Commun. Surveys Tuts.*, vol. 17, no. 4, pp. 1885–1922, 4th Quart., 2015.

[3] G. Fodor, E. Dahlman, G. Mildh, S. Parkvall, N. Reider, G. Miklós, and Z. Turányi, "Design aspects of network assisted device-to-device communications," *IEEE Commun. Mag.*, vol. 50, no. 3, pp. 170–177, Mar. 2012.

[4] M. Klugel, M. He, and W. Kellerer, "Investigation of decision metrics for reuse link selection in device-to-device communication," in *Proc. IEEE 27th Annu. Int. Symp. Pers., Indoor, Mobile Radio Commun. (PIMRC)*, Sep. 2016, pp. 1–6.

[5] M. Klugel and W. Kellerer, "The Device-to-Device reuse maximization problem with power control," *IEEE Trans. Wireless Commun.*, vol. 17, no. 3, pp. 1836–1848, Mar. 2018.

[6] P. Liu, C. Hu, T. Peng, R. Qian, and W. Wang, "Admission and power control for device-to-device links with quality of service protection in spectrum sharing hybrid network," in *Proc. IEEE 23rd Int. Symp. Pers., Indoor Mobile Radio Commun. (PIMRC)*, Sep. 2012, pp. 1192–1197.

[7] H. Sun, M. Sheng, X. Wang, Y. Zhang, J. Liu, and K. Wang, "Resource allocation for maximizing the device-to-device communications underlaying LTE-advanced networks," in *Proc. IEEE/CIC Int. Conf. Commun. China Workshops (CIC/ICCC)*, Aug. 2013, pp. 60–64.

[8] M. Chiang, P. Hande, T. Lan, and C. W. Tan, "Power control in wireless cellular networks," *Found. Trends Netw.*, vol. 2, no. 4, pp. 381–533, 2007, doi: 10.1561/1300000009.

[9] M. Zulhasnine, C. Huang, and A. Srinivasan, "Efficient resource allocation for device-to-device communication underlaying LTE network," in *Proc. IEEE 6th Int. Conf. Wireless Mobile Comput., Netw. Commun.*, Oct. 2010, pp. 368–375.

[10] D. Feng, L. Lu, Y. Yuan-Wu, G. Y. Li, G. Feng, and S. Li, "Device-to-device communications underlaying cellular networks," *IEEE Trans. Commun.*, vol. 61, no. 8, pp. 3541–3551, Aug. 2013.

[11] D. Zhu, J. Wang, A. L. Swindlehurst, and C. Zhao, "Downlink resource reuse for Device-to-Device communications underlaying cellular networks," *IEEE Signal Process. Lett.*, vol. 21, no. 5, pp. 531–534, May 2014.

[12] X. Cai, J. Zheng, and Y. Zhang, "A graph-coloring based resource allocation algorithm for D2D communication in cellular networks," in *Proc. IEEE Int. Conf. Commun. (ICC)*, Jun. 2015, pp. 5429–5434.

[13] S.-A. Ciou, J.-C. Kao, C. Y. Lee, and K.-Y. Chen, "Multi-sharing resource allocation for device-to-device communication underlaying 5G mobile networks," in *Proc. IEEE 26th Annu. Int. Symp. Pers., Indoor, Mobile Radio Commun. (PIMRC)*, Aug. 2015, pp. 1509–1514.

[14] Y. Gu, Y. Zhang, M. Pan, and Z. Han, "Matching and cheating in device to device communications underlying cellular networks," *IEEE J. Sel. Areas Commun.*, vol. 33, no. 10, pp. 2156–2166, Oct. 2015.

[15] R. Yin, G. Yu, H. Zhang, Z. Zhang, and G. Y. Li, "Pricing-based interference coordination for D2D communications in cellular networks," *IEEE Trans. Wireless Commun.*, vol. 14, no. 3, pp. 1519–1532, Mar. 2015.

[16] W. Zhao and S. Wang, "Resource allocation for device-to-device communication underlaying cellular networks: An alternating optimization method," *IEEE Commun. Lett.*, vol. 19, no. 8, pp. 1398–1401, Aug. 2015.

[17] W. Zhao and S. Wang, "Resource sharing scheme for device-to-device communication underlaying cellular networks," *IEEE Trans. Commun.*, vol. 63, no. 12, pp. 4838–4848, Dec. 2015.

[18] T. D. Hoang, "Resource allocation for D2D communication underlaid cellular networks using graph-based approach," *IEEE Trans. Wireless Commun.*, vol. 15, no. 10, pp. 7099–7113, Oct. 2016.

[19] T. Huynh, T. Onuma, K. Kuroda, M. Hasegawa, and W.-J. Hwang, "Joint downlink and uplink interference management for device to device communication underlaying cellular networks," *IEEE Access*, vol. 4, pp. 4420–4430, 2016.

[20] S. Maghsudi and S. Stanczak, "Hybrid Centralized–distributed resource allocation for device-to-device communication underlaying cellular networks," *IEEE Trans. Veh. Technol.*, vol. 65, no. 4, pp. 2481–2495, Apr. 2016.

[21] R. Yin, C. Zhong, G. Yu, Z. Zhang, K. K. Wong, and X. Chen, "Joint spectrum and power allocation for D2D communications underlaying cellular networks," *IEEE Trans. Veh. Technol.*, vol. 65, no. 4, pp. 2182–2195, Apr. 2016.

[22] H. Zhang, L. Song, and Z. Han, "Radio resource allocation for device-to-device underlay communication using hypergraph theory," *IEEE Trans. Wireless Commun.*, vol. 15, no. 7, pp. 4852–4861, Jul. 2016.

[23] J. Hu, W. Heng, Y. Zhu, G. Wang, X. Li, and J. Wu, "Overlapping coalition formation games for joint interference management and resource allocation in D2D communications," *IEEE Access*, vol. 6, pp. 6341–6349, 2018.

[24] P. S. Bithas, K. Maliatsos, and F. Foukalas, "An SINR-aware joint mode selection, scheduling, and resource allocation scheme for D2D communications," *IEEE Trans. Veh. Technol.*, vol. 68, no. 5, pp. 4949–4963, May 2019.

[25] J. Li, "D2D communication mode selection and resource optimization algorithm with optimal throughput in 5G network," *IEEE Access*, vol. 7, pp. 25263–25273, 2019.

[26] M. Klügel, "Operation and control of device-to-device communication in cellular networks," Ph.D. dissertation, Dept. Elektrotechnik Informationstechnik, Tech. Univ. Munich, Munich, Germany, 2018. [Online]. Available: http://mediatum.ub.tum.de/node?id=1425301

[27] M. Klugel and W. Kellerer, "Poster abstract: Semi-decentralized interference management in D2D-enabled cellular networks," in *Proc. IEEE Conf. Comput. Commun. Workshops*, Apr. 2018, pp. 1–2.

[28] C. Wan Sung, "Log-convexity property of the feasible SIR region in power-controlled cellular systems," *IEEE Commun. Lett.*, vol. 6, no. 6, pp. 248–249, Jun. 2002.

[29] C. W. Tan, D. P. Palomar, and M. Chiang, "Exploiting hidden convexity for flexible and robust resource allocation in cellular networks," in *Proc. 26th IEEE Int. Conf. Comput. Commun.*, Dec. 2007, pp. 964–972.

[30] S. Stanczak, *Fundamentals Resource Allocation Wireless Networks: Theory Algorithms*, 2nd ed. Berlin, Germany: Springer, 2009.

[31] J. F. Benders, "Partitioning procedures for solving mixed-variables programming problems," *Numerische Math.*, vol. 4, no. 1, pp. 238–252, Dec. 1962.

[32] A. M. Geoffrion, "Generalized benders decomposition," *J. Optim. Theory Appl.*, vol. 10, no. 4, pp. 237–260, Oct. 1972.

[33] C. Floudas, *Nonlinear and Mixed-Integer Optimization: Fundamentals and Applications* (Topics in Chemical Engineering). London, U.K.: Oxford Univ. Press, 1995.

[34] G. J. Foschini and Z. Miljanic, "A simple distributed autonomous power control algorithm and its convergence," *IEEE Trans. Veh. Technol.*, vol. 42, no. 4, pp. 641–646, Nov. 1993.

[35] N. Bambos, S. C. Chen, and G. J. Pottie, "Channel access algorithms with active link protection for wireless communication networks with power control," *IEEE/ACM Trans. Netw.*, vol. 8, no. 5, pp. 583–597, Oct. 2000.

[36] R. D. Yates, "A framework for uplink power control in cellular radio systems," *IEEE J. Sel. Areas Commun.*, vol. 13, no. 7, pp. 1341–1347, Sep. 1995.

[37] D. Kim, "On the convergence of fixed-step power control algorithms with binary feedback for mobile communication systems," *IEEE Trans. Commun.*, vol. 49, no. 2, pp. 249–252, Feb. 2001.

[38] H. W. Kuhn, "The hungarian method for the assignment problem," *Nav. Res. Logistics Quart.*, vol. 2, nos. 1–2, pp. 83–97, Mar. 1955.

[39] J. Munkres, "Algorithms for the assignment and transportation problems," *J. Soc. Ind. Appl. Math.*, vol. 5, no. 1, pp. 32–38, Mar. 1957.

[40] *Results and Tool-Chain for, Semi-Decentralized Interference Aware Scheduling in D2D-Enabled Cellular Networks*. Accessed: Jul. 20, 2020. [Online]. Available: https://mediatum.ub.tum.de/1483807

[41] P. Kyösti. (2007). *WINNER II Channel Models*. [Online]. Available: http://www.ist-winner.org/WINNER2-Deliverables/D1.1.2v1.1.pdf

[42] *Evolved Universal Terrestrial Radio Access (E-Utra); Radio Frequency (RF) System Scenarios*, document TR 36.942, 3rd Generation Partnership Project, Sep. 2012.